POWER STORAGE IN D OCEAN

D2.2. WP2 Engineering Design which includes fabrication drawings, bill of materials, schemes for the SMES superconducting magnet, cryogenic system, and the converter.

Document Information	
Deliverable	2.2
Lead Beneficiary	CYCLOMED TECHNOLOGIES
Type:	R -
Work Package	WP2 ESS 1: SMES Superconducting Magnetic Energy storage for marine applications.
Date	30/06/2024

Dissemination level

Dissemination Level	
SEN: Sensitive, limited under the conditions of the Grant Agreement	X

History

Version	Date	Reason	Revised by
1	26/05/2024	First draft	
2	26/06/2024	Final Version	
3		Peer reviewed	
4		Final version submitted	

Author List

Organization	Name	Contact Information
CYCLOMED	Carlos Hernando	c.hernando@cyclomed.tech
CYCLOMED	Carlos Gil	c.gil@cyclomed.tech
ANTEC	Rafael Iturbe	r.iturbe@antecsa.com
ANTEC	Borja Lopez	b.lopez@antecsa.com
CIEMAT	Luis Gª-Tabarés	Luis.garcia@ciemat.es

Disclaimer

TABLE OF CONTENTS

1. EXECUTIVE SUMMARY

The POSEIDON project's Deliverable 2.2 document focuses on the engineering design and implementation of a Superconducting Magnetic Energy Storage (SMES) system specifically for marine applications. As part of the broader initiative to electrify the economy, the maritime transport sector is experiencing significant transformations, particularly in the management of power quality and flow within increasingly complex ship grids. The integration of Energy Storage Systems (ESS) is vital to addressing these new challenges. However, conventional high-energy density ESS, such as Li-ion batteries, often fall short in meeting the specific power needs of certain maritime applications. For example, short river ferries, which operate with numerous duty cycles, require high specific power systems that traditional batteries cannot efficiently provide.

This document elaborates on the initial design report (D2.1), highlighting the importance of SMES as a viable solution to these power management issues. The report discusses the limitations of Li-ion batteries and underscores the necessity for advanced ESS technologies that can offer high specific power. The unique attributes of SMES make it particularly suitable for maritime applications where quick and efficient power delivery is essential.

In terms of technology selection, the project has chosen 2G HTS Tape from Shanghai superconductors due to its high critical temperature, which reduces the power required by the refrigeration system. This material also boasts favorable electromagnetic and mechanical properties and is economically advantageous. The solenoidal topology, composed of 12 double-pancake coils, was selected for its ease of assembly, fabrication, and scalability due to its modular design. The refrigeration system employs a Cryogenic Supply System (CSS) that allows for effective heat extraction, circulating gas through the magnet rather than relying on conduction. The power and control system design features a Voltage Source Converter (VSC) with a commercial bipolar power supply and a DC-DC chopper, allowing for independent control of active and reactive power while maintaining a low Total Harmonic Distortion (THD). The targeted energy range for the SMES is 150-250 kJ, with the initial development aiming for 275 kJ at an operating temperature of 4.2K.

The document details the iterative development process of the SMES prototypes. Prototype 0 focused on the initial design and fabrication, emphasizing the characteristics of the HTS tape, electromagnetic and mechanical design, followed by rigorous testing in liquid nitrogen (LN2) and liquid helium (LHe). Prototype 1 further refined these designs, incorporating improved electrical connections and extensive testing to ensure reliability and performance.

Overall, the document outlines the comprehensive planning and iterative development process, including engineering drawings and annexes for future reference. This project, funded by the European Union, reflects the authors' views and emphasizes the collaborative effort needed to advance the implementation of SMES systems in the maritime sector.

2. INTRODUCTION

2.1. SUMMARY OF DESIGN REPORT (D2.1)

The electrification of the economy is a reality that is impacting the transportation sector, including maritime transport. Ship grids are evolving in complexity, developing new issues such as complex control of the power quality, and power flow. Some of these arising

problems can be addressed with the addition of Energy Storage Systems (ESS) in the ship microgrid. We realize the following:

1. The integration of high energy density ESS, such as Li-ion batteries, in ships is rapidly improving, however there are specific situations that cannot be addressed by this type of ESS, and there is need for high specific power systems. It is the case, for example, of a short river ferry which has a power profile with a high number of duty cycles.
2. Being a novel industry in the maritime sector, there is little regulation on ESS, and most of it is focused on electrochemical batteries. Therefore, the ESS designer must work with regulators, and/or provide their insights, in order to address the marinization of these novel technologies. We have identified the most relevant existing directives that will establish the guidelines and minimum conditions for correct and safe integration of the SMES on-board.
3. According to state-of-the-art information and use case we have established a range of energy and power values which are attractive for an SMES with on-board application. For the SMES developed in POSEIDON we are targeting the low range of energy, limiting this first development to 150-250 kJ.

Among the technological alternatives in the development of a SMES, Table 1 provides a summary of the selected technologies POSEIDON SMES.

Table 1. Technological selections of POSEIDON SMES

	Selection	Description
SC Material	**2G HTS Tape**	HTS technology selected due to its **High critical temperature:** Less power required by the refrigeration system. Easier to remove AC losses. Shanghai superconductors as tape provider: best EM and good mechanical properties. Best economics. Partners have worked with them in the past which reduces risks.
Topology	**Solenoidal**	Solenoidal arrangement made of 12 double-pancake coils. This option is **easy to assemble** and easy to fabricate. **Scalability due to its** modularity.
Refrigeration	**Cryogenic Supply System (CSS)**	Flow refrigeration with CSS. Selected for its affordability, and capacity to extract **heat very close from where it is produced** (the tape) since the gas is circulated through the magnet and not removed from conduction.
PCS	**VSC & DC-DC chopper**	Selected a simplified version of the VSC with a commercial bipolar power supply connected to the grid and a chopper. Allows **Independent control of the Active and Reactive Power**. The overall THD can be quite small.

More specifically Table 2 provides the main parameters of the conceptual design for the POSEIDON SMES.

Table 2. Main Parameters of Poseidon SMES

	Parameter	Value
SC material	Material	2G HTS Tape

	Supplier	Shangai Superconductors
	Dimensions	4.8 mm width & 0.2-0.25 mm thickness Cu laminated
SC coil	Internal radius	86 mm
	Cross section	49x10 mm^2
	Turns	144 per coil (200 m. of tape)
Magnet	Nº of Double pancakes	12
	Topology	Solenoidal
	Inductance	1.68 H
	Nominal current	457A @4.2K (220A @20K) (80% of critical current)
Cooling system	Operating temperature	4.2K@LHe bath (20K in operation)
Power and control system	Topology	Voltage Source Converter
SMES	Energy	275 kJ (@ 4.2K)

2.2. TECHNOLOGY CHALLENGES

2.2.1. HTS TECHNOLOGY CHALLENGES

The selection of High Temperature Superconductivity (HTS) as the superconducting material represents a bold and forward-looking choice. While the technology is relatively nascent, its potential advantages are significant. Nevertheless, this choice is accompanied by a set of challenges. In the initial months of design and testing, we have identified the following challenges associated with HTS magnets:

- **Mechanical degradation**: Mechanical disturbances, frictional conductor motion, due to stress accumulation: 1) cool down and 2) coil charging, can cause mechanical degradation to HTS magnets. The anisotropy of the mechanical properties of HTS tapes: tensile strength in the transverse direction (10-100MPa) and cleavage and peel strength (1 MPa) are typically the limiting factors.

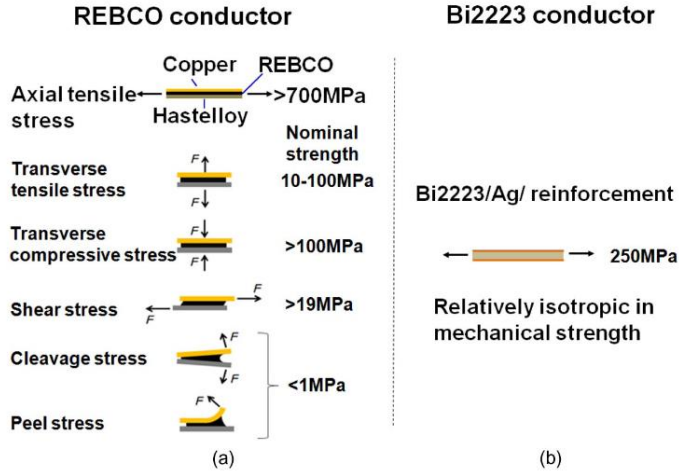

Figure 1. Stress limits in different direction for a REBCO tape

- **Screening currents**: These currents are induced in the superconducting tapes to resist the penetration of magnetic fields into the conductor. In HTS magnets, the shielding current distribution plays a crucial role in determining the mechanical responses, particularly the hoop stress and strain distributions, and also the magnetic field distribution. The shielding current is responsible for creating significant mechanical stresses in the coil, which can lead to reduced performance and lifetime.

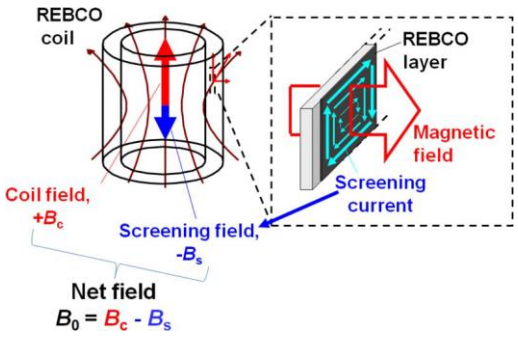

Figure 2. The radial component of the magnetic field penetrates a wide area of an HTS tape conductor, inducing a screening current induced magnetic field, Bs. The net central magnetic field is equal to Bc–Bs. Figure from [1]

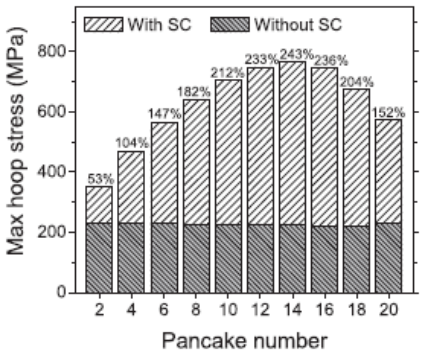

Figure 3 Maximum local hoop stresses in pancakes based without accounting for Screening Currents (Max. Stress of 225MPa) and accounting for SCs (Max. Stress of 775MPa). Figure from [2]

- **Stability and protection**: The normal zone propagation velocity in HTS coils is several orders of magnitude lower than in Low-Temperature Superconducting (LTS) coils. This makes it difficult to protect HTS magnets from thermal runaways and requires additional measures to prevent damage.
- **AC losses:** AC losses occur when a superconductor is exposed to alternating electromagnetic fields, which cause energy dissipation and heat generation within the material. This heat must be removed from the low-temperature environment by a refrigerator, which is generally very low efficient. If the heat is not removed and the magnet heats up, it can cause a thermal runaway or quench. Due to the geometry of the tapes AC losses in REBCO tapes are specially significant when compared to LTS or other HTS solutions.

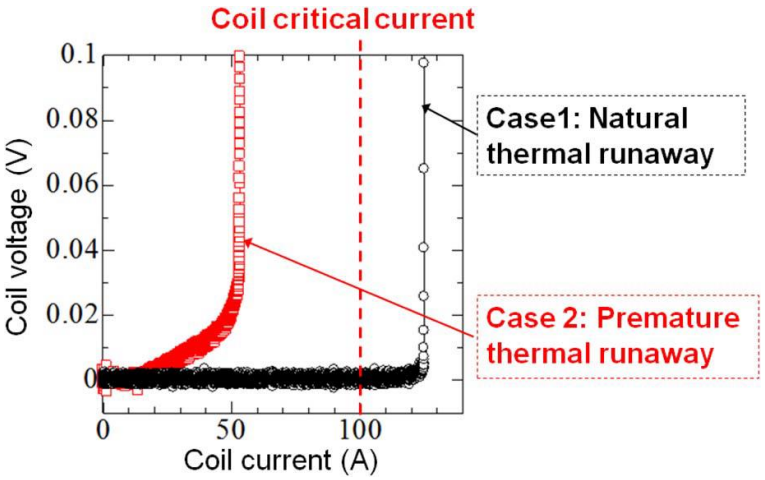

Figure 4. Two types of thermal runaway for HTS magnets. Case 1; a natural thermal runaway which emerges above the coil critical current. Case 2; a premature-thermal runaway that suddenly occurs at a current below the coil critical current, seen in particular for REBCO coils. Figure from [1]

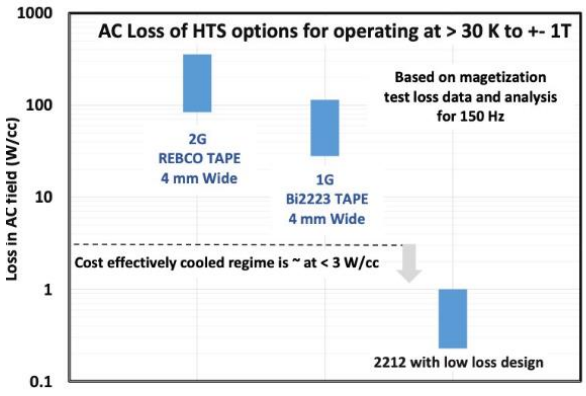

Otto, *Low Temp. Supercond. Workshop* (2022)

Figure 5 Heat generated per centimeter cube of superconductor for different HTS technologies: REBCO, and BSCCO.

2.2.2. MANUFACTURING CHALLENGES

Winding & Impregnation: Superconducting wires must be wound with high precision to ensure uniform magnetic fields and avoid mechanical stresses that could damage the brittle superconducting material. Furthermore, proper winding techniques are essential to prevent quenching since uneven winding can create hotspots, leading to quenching.

After winding, the coils need to be impregnated with resin or other materials to fix the wires in place and provide mechanical stability. Ensuring complete impregnation without voids is crucial, as voids can lead to quenching and reduced performance. The impregnating material must be compatible with the superconducting wire and the operating environment. It must withstand cryogenic temperatures and maintain its properties without degrading over time. In addition, the materials used for impregnation must have a thermal contraction coefficient similar to that of the superconductor to prevent stress and potential damage when cooled to cryogenic temperatures.

Electrical joints: Electrical joints between superconducting wires or cables must have extremely low resistance to maintain superconducting properties. Even a small amount of resistance can generate heat and cause quenching. These joints must remain stable and maintain their properties at cryogenic temperatures. The materials used must not degrade or change their electrical characteristics when cooled.

Creating reliable, low-resistance joints is technically challenging. Techniques such as soldering, welding, or using mechanical clamps require high precision and control to avoid introducing defects or contaminants that could increase resistance.

Current leads: The current leads must handle high currents without significant resistive losses. This requires careful design and material selection to ensure efficient current transfer. Materials with low thermal conductivity but good electrical conductivity, like high-purity copper or HTS materials, are preferred.

Current leads need to be mechanically strong to handle thermal contraction and expansion during cooling and operation. This ensures they remain intact and maintain good electrical contact without introducing stress-induced failures.

2.3. UPDATED PLANNING

To correctly addressed the identified challenges the following modifications has been made to the initial work plan:

- Advanced Modeling Techniques: to correctly understand and evaluate the phenomena associated with high temperature superconductivity it is necessary to develop models that correctly capture the associated physics. In the first months of the design phase more effort will be put in these tasks.
- Early prototyping: in order to evaluate the developed models and the effect of the detected challenges in the technology it is imperative to develop test benches and do in-scale experimental validation. For that reason, we have advanced the fabrication of scaled HTS coils from the initial work plan. The new work plan consisted of:
    - Design, Manufacture and Test Prototype 0 (August 2023-March 2024): this is a 0.5-scaled coil from the final versions. This coil will allow us to evaluate and measure the key variables for model validation.
    - Design, Manufacture and Test Prototype 1: (March 2024-July 2024): this will be an actual version of the final SMES modules and will be integrated in the SMES if all tests are successful.
- Delay cryogenic activities: Since the electromagnetic design, and fabrication processes require more intense effort during the design phase the cryogenics of the system will be simplify in the initial tests. The final design and fabrication of the final system will be delayed by 6-9 months without affecting the total length of the project. The final drawings will be included in the next deliverable (D2.3)

Fundamental of HTS magnets	Mitigation	Status
Screening Currents	- Advanced simulation tools: use of latest Multiphysics FEM solvers - Early prototyping: develop scaled prototypes to validate the model - Progressive testing: increase number of test to detect and correct new challenges.	Develop EM models that capture SC and their effect. Good comparison against S-o-A results. More experimental validation is needed
Mechanical degradation		Developed scaled prototypes and tested in real operating conditions. No sign of degradation in first prototypes.
AC losses		Develop EM simulation that correctly predicts AC losses when compared to S-o-A results. Development of test benches, and early experiments but need
Stability & Protection		Currently developing coupled EM and thermal models.
Manufacturing		
Winding & Impregnation	- Early prototyping: develop scaled prototypes to validate the model - Progressive testing: increase number of test to detect and	Manufacture a 0.5x scale prototype. No internal weak points detected
Joints: Soldering & Mechanical		Detected challenge to decrease joint resistance. Launched a experimental campaign.
Current Leads		Detected challenge to transport high currents, which increase

	correct new challenges	heat generation and can lead to quenches. Launched campaign of experiments.
Marinization		
Mechanical	- Regulations and normative analyzed. Established main design constraints	Incorporate design constraints in the design process. Need to stablish a procedure to test constraints and to track them during testing
Electromagnetic		

In the following sections the design, fabrication and testing of the prototypes 0 and 1 will be explained including the engineering drawings as an annex.

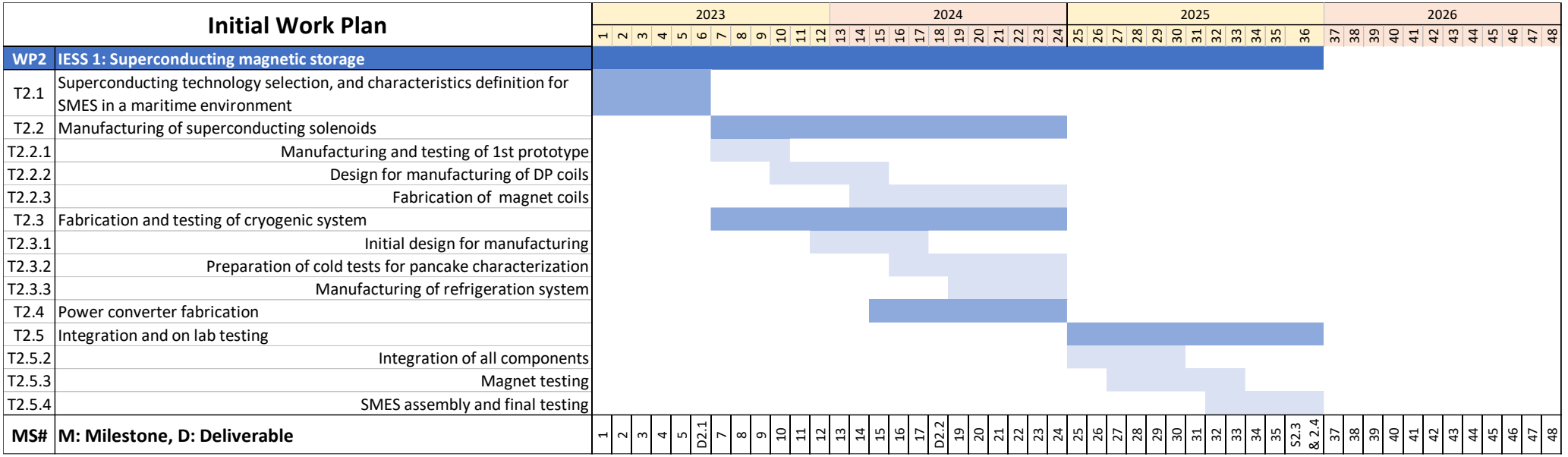

Figure 6. Work plan at the start of the project – January 2023

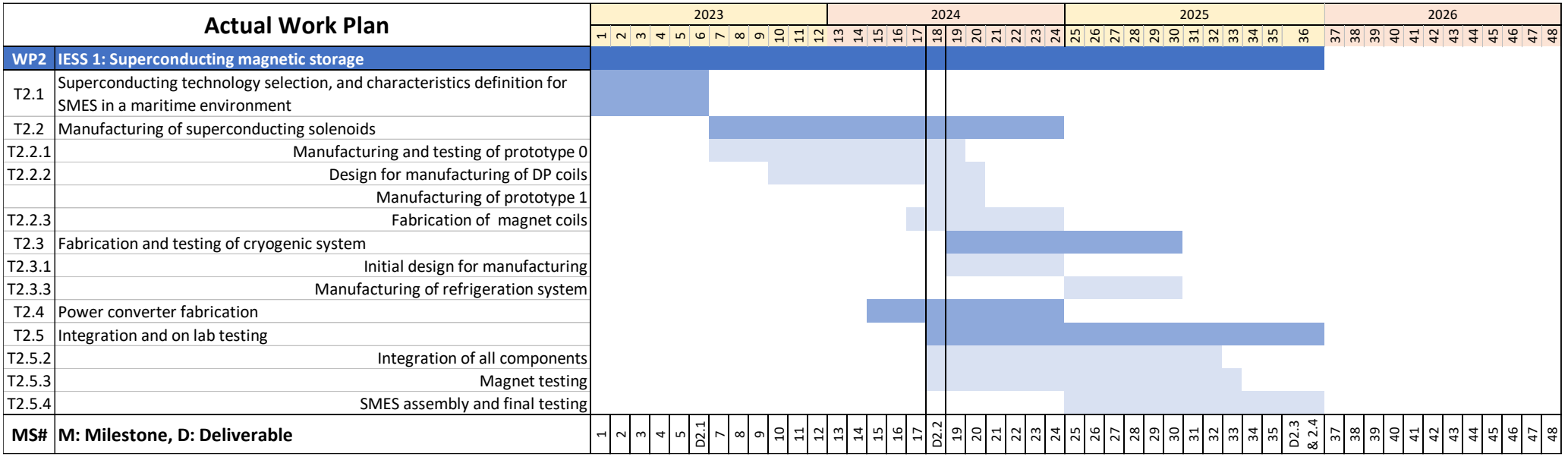

Figure 7. Updated Work plan – June 2024

3. SUPERCONDUCTING COIL MANUFACTURING PROCESS

The manufacturing process of superconducting coils for the SMES (Superconducting Magnetic Energy Storage) system involves a series of carefully controlled steps to ensure optimal performance and reliability. This section outlines the procedures and technologies employed in the creation of these advanced coils. Starting with the winding of HTS (High-Temperature Superconductor) tapes, the process includes precise control of winding tension, careful execution of layer jumps to prevent degradation, and the application of resin to bond the coil layers. Each stage is critical to maintaining the superconducting properties and mechanical integrity of the coils, ultimately contributing to the efficiency and durability of the SMES system. The figures depicted in this section shows the actual manufacturing process that the Prototype 0 coil went through.

3.1. WINDING MACHINE

A winding machine was installed at ANTEC's premises for the manufacturing of coils. The machine consists of two reels that store the conductor needed for coil production. These reels rotate around the winding mandrel in opposite directions. The winding tension applied to the conductor is controlled throughout the entire process.

Superconducting HTS tapes must be wound into "double pancake" coils with two layers, which can be wound either sequentially or simultaneously. These coils are wound using a simultaneous winding technique with two rotating spools.

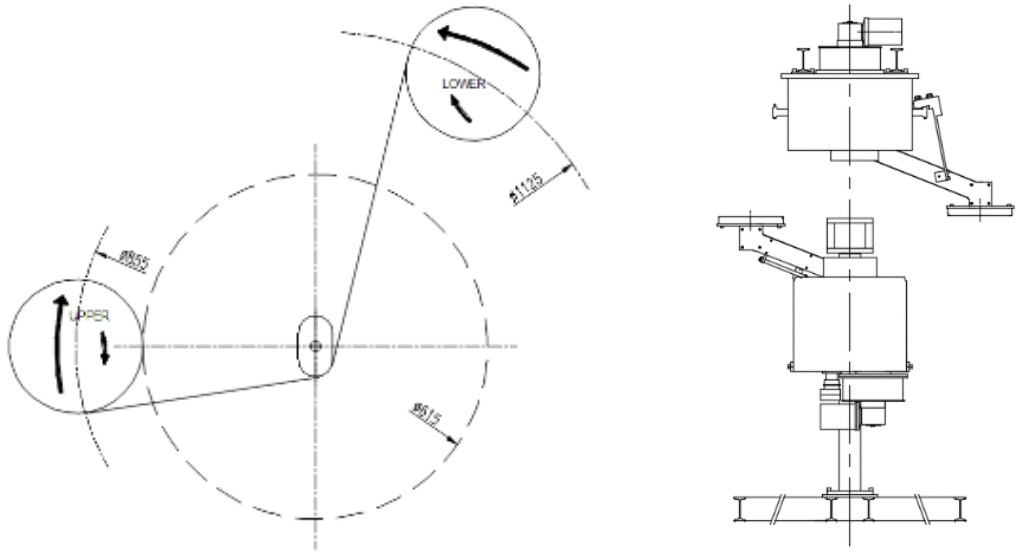

Figure 8 Coil winding machine scheme

Due to the fragility of the conductor and to avoid degradation the superconductor damaging its superconducting properties, certain precautions have to be taken into account. One of them is, to reduce the mechanical efforts in the tape when winding is placing the HTS side of the tape facing outwards of the coil, while maintaining a bending radius bigger than 30 mm.

3.2. WINDING TOOL

To achieve the dimensions of the coils a winding tool was designed. The winding tool has to fix the position of the tape while winding, guide the HTS to its correct position and, finally, allow the extraction of the coil after the resin curing process.

It consists of a circular mandrel of fiber glass, G11, around which the tape is wound.

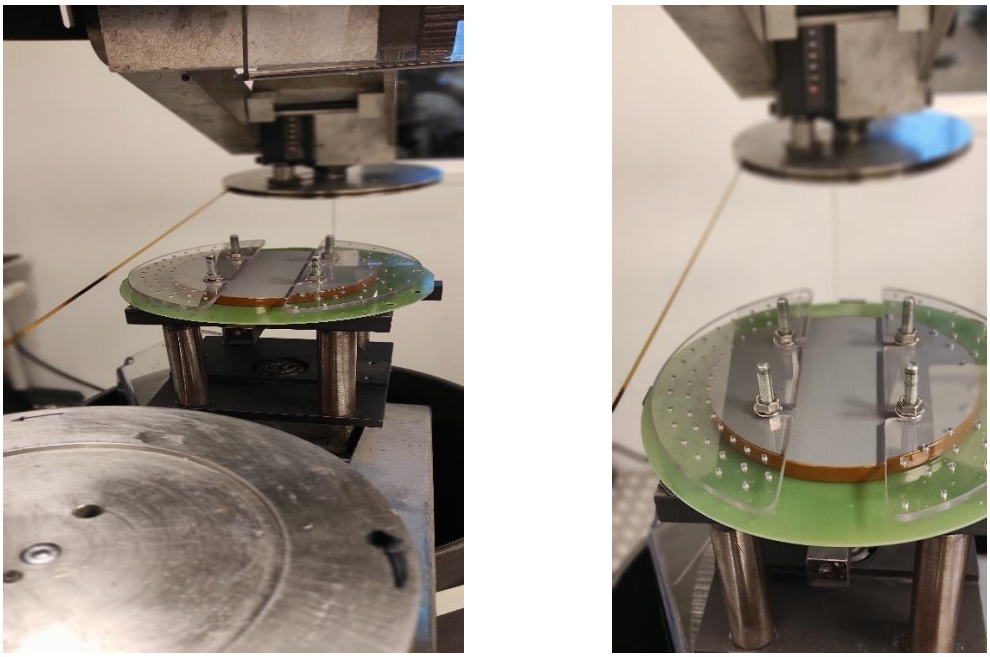

Figure 9 Tool placed in the winding machine

3.3. HTS TAPE

The HTS tape is composed of 4 different layers, see next figure. The Superconducting material is brazed on top of a stainless-steel substrate and surrounded by two copper-brazed layers. Finally, the conductor is insulated by means of a Kapton tape.

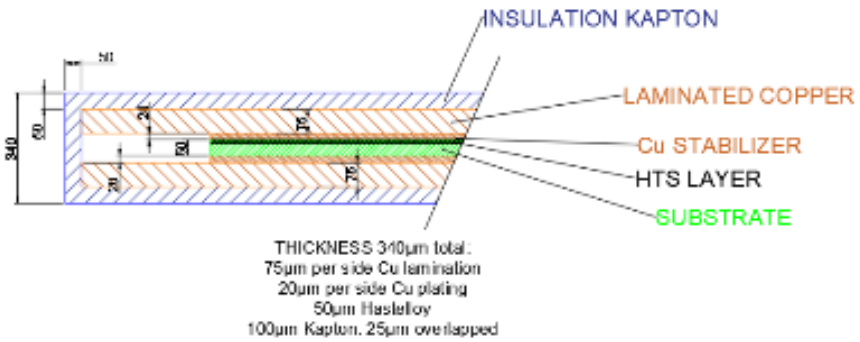

Figure 10 HTS Dimensions and composition

3.4. LAYER JUMPS

Since the outlet and inlet electrical coil connections need to be on the outer perimeter of the coil, the double pancake geometry was chosen. This design involves a layer jump in the middle of the required conductor length. Due to the fragility of the HTS tape, the layer jump must be executed carefully to avoid degrading the tape's superconducting properties. Specifically, small bending radii must be avoided.

Additionally, the jump must be easily reproducible to ensure geometric consistency across all coils. Therefore, the execution of the layer jump must be rigorously tested to confirm that it does not cause any degradation.

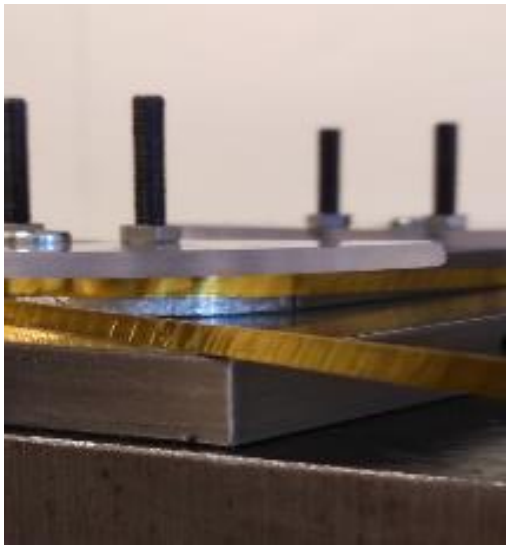

Figure 11 Layer Jumps

3.5. COIL WINDING

As explained above, the winding is performed by turning two spools simultaneously around the mandrel the number of turns required for the coil. Each of the spools feeds each layer, top and bottom, of the double pancake.

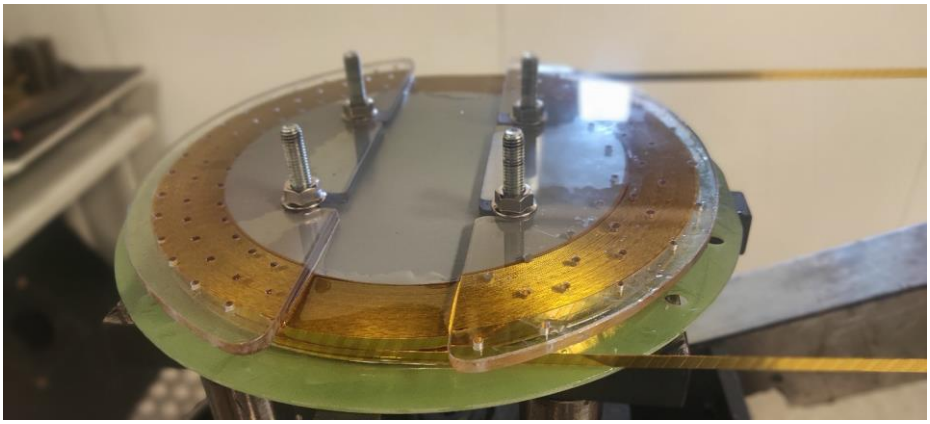

Figure 12 Coil Winding

3.6. BRAZING

It is important to maintain the temperature below 300 °C to prevent degradation of the tape characteristics. Additionally, all cut areas at the ends of the tapes must be properly covered. To define and validate the brazing procedures, various tests were performed.

Figure 13 Brazing stress

When the coil is finished the electric connections of the coil are brazed.

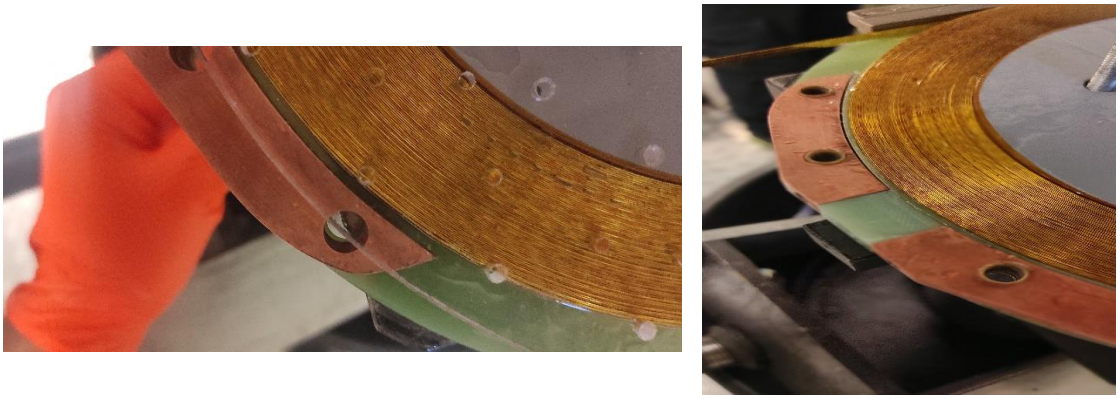

Figure 14 Terminals brazing

3.7. IMPREGNATION

Due to the small gaps between the coil turns, vacuum impregnation is not considered the best solution. Therefore, the wet winding procedure was selected. This method involves applying resin while winding, ensuring that all the different turns and layers of the coil are bonded together after the curing process. The resin used is Araldite F, an epoxy commonly employed in cryogenic applications.

After winding and brazing the terminals, the coil is placed in an impregnation tool and cured in an oven at 120 °C for 2 hours.

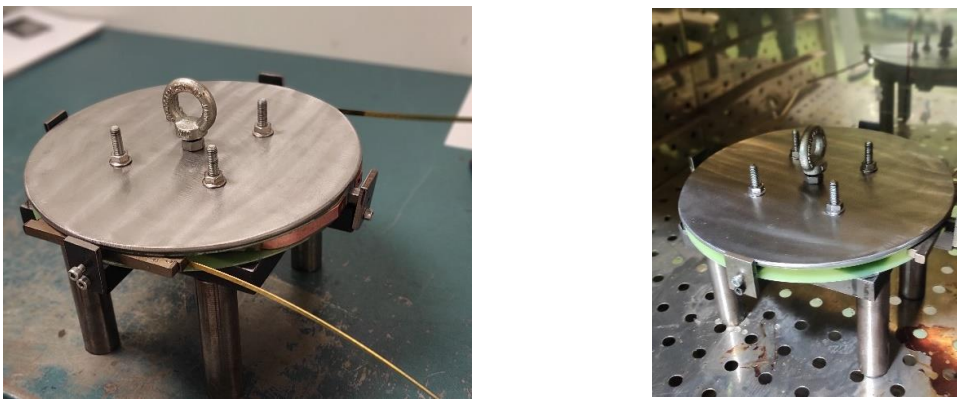

Fig. 1. Curing tool

4. PROTOTYPE 0: PK0

4.1. DESIGN

4.1.1. HTS TAPE CHARACTERISTICS

TABLE III provides a comparison of the main mechanical properties of each HTS from the selected suppliers. The selected supplier for prototype 1 is Shanghai SC.

TABLE III Main mechanical properties of the superconducting tape provided by Theva, Shangai superconductors and Sumitomo.

PROPERTIES	Theva Pro-Line	Shanghai SC 2G REBCO	Sumitomo
Substrate	50 µm Hastelloy	30-50 µm Hastelloy	Type H - No reinforcement Type HT - Reinforced (SS, Copper, Nickel)
Buffer Layer	MgO	MgO + Others	-
Superconductor	GdBaCuO	REBCO 2G (GbBa2Cu3O7/EuBCO/YGdBCO)	BSSCO
Width	12 / 6 / **4** / 3 mm	10/ **4** / 3.3/ mm	4.5+-0.1 mm
Average thickness	0.11 + 0.05/0.1 mm Cu foil (laminated)	0.065-0.095 +- 10% mm Cu Plating	Type H - 0.23 +-0.01 mm.
		0.205-0.255 +-10% mm Cu lamination	Stainless Steel 0.29 +-0.02 mm.
	0.11 + 0.01/0.02 Cu surround (plated)	0.215 +-10% mm SS304 lamination	Copper Alloy 0.34 +- 0.02 mm.
			Nickel alloy 0.31 +- 0.03 mm
Minimum Bending Radius	20 mm	6-7 mm CU Plating	Type H - 80 mm.
			Stainless Steel 60 mm
		7-10 mm Cu Lamination	Copper Alloy 60 mm
		7-10 mm SS304 Lamination	Nickel alloy 40 mm
Maximum Handling Force	50 N for 12mm tape	-	Wire tension 80 N
			Wire tension 230 N
			Wire tension 280 N
			Wire tension 410 N
Maximum Rated Stress	165 to 500 MPa	100 MPa Cu Plating	Stainless steel - 20um : 270 MPa tensile strength 0.4% critical strain
		300-400 MPa Cu Lamination	Copper - 50 um: 250 MPa tensile strength 0.3% critical strain
		>700 MPa SS304 Lamination	Nickel alloy - 30um: 270 MPa tensile strength 0.4% critical strain
Piece Length (max)	25 to 200 m	< 1000 * m	Type H - < 1500 m.
			Type HT - < 500 m.
Insulation	Not provided	2 Kapton 25 µm width tapes overlapped	-
Price	32 €/m (depends on stock) + packaging & shipping for 100/200	25-30 $/m \\ 23-28 €/m for S+ (medium grade) and a length 100	20-30 $/m \\ 23-28 €/m

	m (short lengths for their production)	m. Double the length 40-50% more expensive.

The properties of an HTS tape are highly anisotropic, since it's made of stacked layers of different materials. The layers have been modeled in Ansys, and the equivalent properties for the composite material have been obtained, which have been used for the electromagnetic and mechanical modeling shown in the following sections.

TABLE IV. Properties for each layer of the HTS tape

	Layer	Thickness (micron)	Width (mm)	Area(micron mm)	Young Modulus(Gpa)	Ei Ai	ti / Ei
External Support	Kapton	50	4.8	240	5.3	1272	9.4
	Cu Lamination	75	4.8	360	138.6	49896	0.5
	PbSn (Soldering)	10	4.8	48	45	2160	0.2
Main Body	Cu Stabilizer	10	4.8	48	138.6	6652.8	0.1
	Silver	1.6	4.8	7.68	91.1	699.648	0.0
	REBCO	1.6	4.8	7.68	170	1305.6	0.0
	Buffer	0.2	4.8	0.96	280	268.8	0.0
	Hastelloy	50	4.8	240	212	50880	0.2
	Silver	2	4.8	9.6	91.1	874.56	0.0
	Cu Stabilizer	10	4.8	48	138.6	6652.8	0.1
External Support	PbSn (Soldering)	10	4.8	48	45	2160	0.2
	Cu Lamination	75	4.8	360	138.6	49896	0.5
	Kapton	50	4.8	240	5.3	1272	9.4
	Total:	345.4		1658			
	Datasheet:	340		Módulo Young Long	104.94		
				Módulo Young Tran:	16.59		

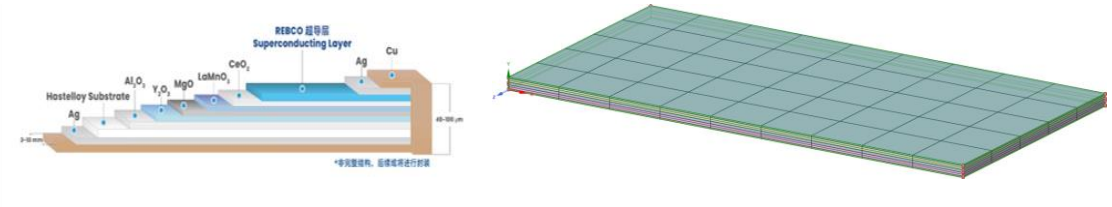

Figure 15. HTS tape model in material designer from Ansys

The equivalent coefficient of thermal expansion of the HTS tape is shown in Figure 16, the X and Z tape, the longitudinal direction, is similar to that of copper. In the transverse direction the CTE is significantly lower.

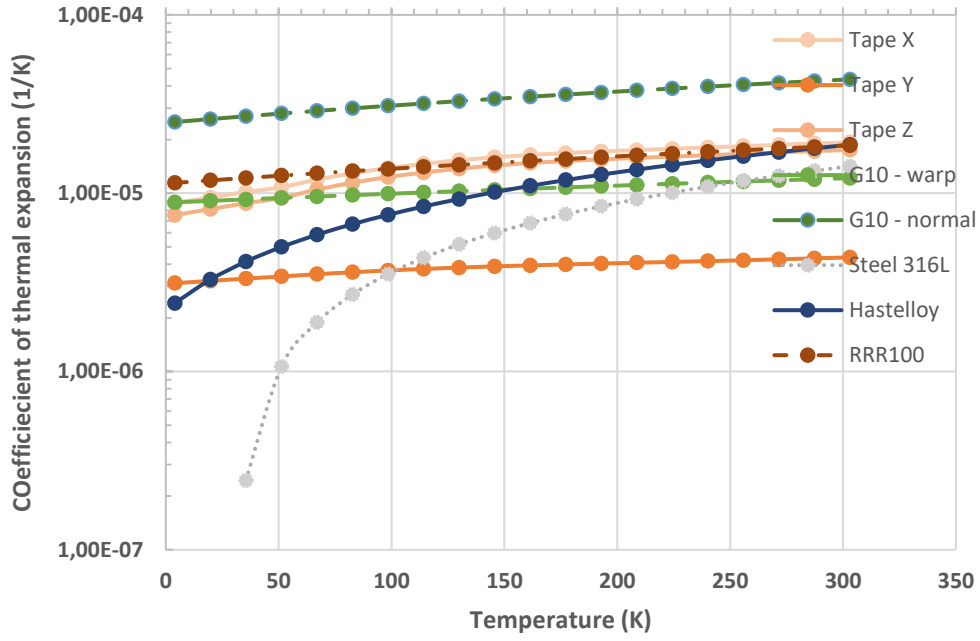

Figure 16. Coefficient of thermal expansion for HTS tapes in 3 axis and other relevant materials.

4.1.2. ELECTROMAGNETIC DESIGN

The electromagnetic design of the prototype coil is carried out as follows: Each point of the coil has a specific value of critical current associated with it. This value depends on the magnitude of the field, temperature, and field angle.

For the determination of the coil's critical current, an electromagnetic FEM model was developed to estimate the magnetic field and angle in every point of the coil. Having identified the most critical point, the one with worst combination of magnetic field amplitude and field direction, the load curve is constructed relating the magnetic field and current.

Figure 17 shows the load curve of the magnet and the critical current, which is the intersection of the load curve with the current density curves, at different temperatures.

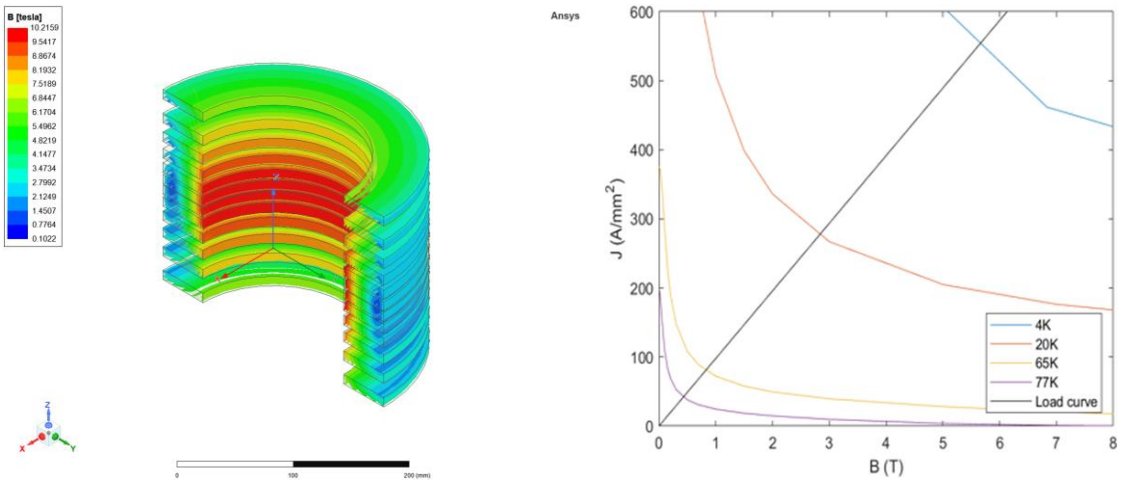

Figure 17. Load curve of PK0: magnetic field vs current density at different temperatures of coil PK0

The theoretical V-I curve at 77.5 K (Liquid Nitrogen temperature) of the coil is shown in Figure 18 a). This curve will be validated experimentally. The black horizontal line indicates the quench limit, above that value the magnet is considered to have lost its superconducting state. Figure 18 b) lists the values of the critical current at different temperatures.

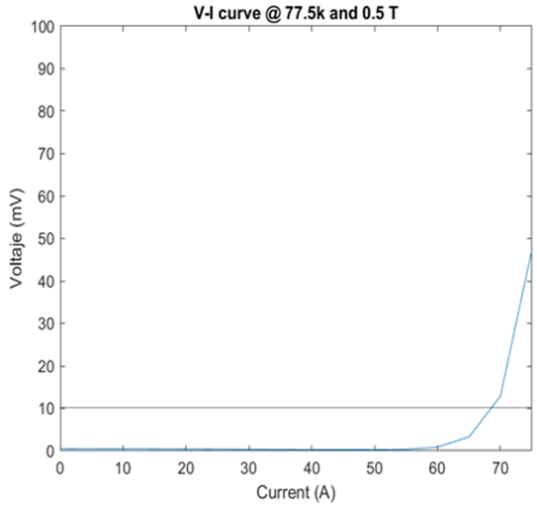

Temperature	Ic (A)	Iop (A)
77.5 K	69.1	55.29
65 K	131.6	105.3
20 K	449.6	359.7
4.2	896.6	717.3

Figure 18. a) V-I curve of PK0 coil at 77K. b) Temperature and critical current (under 1uV/cm criterion) for different temperatures

4.1.3. MECHANICAL DESIGN

The mechanical design of an HTS coil has 2 main components, first the stresses induced due to the cooling of the coil, and second, the electromagnetic forces induced by the magnetic field in the conductor.

Thermal stresses

The prototype 0 coil has an inner mandrel made of soft iron; this material has a lower CTE than the HTS tape. Due to CTE differences, mechanical stress will be induced in the coil during cool down. For reference, TABLE V shows the mean thermal expansion for materials typically used in cryogenics.

TABLE V. Mean Linear Thermal Expansion Data of Selected Materials

Material	T [K]				
	20	80	140	200	973†
Aluminum	−0.415*	−0.391	−0.312	−0.201	—
Brass (70Cu-30Zn)	−0.369	−0.337	−0.260	−0.163	+1.30
Bronze	−0.330	−0.304	−0.237	−0.150	+1.33
Copper	−0.324	−0.300	−0.234	−0.148	+1.3
Nickel	−0.224	−0.211	−0.171	−0.111	—
Silver	−0.409	−0.360	−0.270	−0.171	+1.50
Stainless steel 304	−0.306	−0.281	−0.222	−1.40	+1.32
Epoxy	−1.15	−1.02	−0.899	−0.550	—
G-10 (warp)	−0.241	−0.211	−0.165	−0.108	—
G-10 (normal)	−0.706	−0.638	−0.517	−0.346	—
Phenolic (normal)	−0.730	−0.643	−0.513	−0.341	—
Teflon (TFE)	−2.11	−1.93	−1.66	−1.24	—
Nb_3Sn	−0.171	−0.141	−0.102	−0.067	+0.55
Cu/NbTi wire	−0.265	−0.245	−0.190	−0.117	—
Solder (50Sn-50Pb)	—	−0.510	−0.365	−0.229	—

The presence of an inner mandrel can induce mechanical stress that should be carefully checked. Low contraction materials are usually preferred, but those are typically not electromagnetically compatible (stainless steel, copper…), and other alternative innovative materials does not have their properties tested at cryogenic temperatures, therefore the selection is narrow.

Electromagnetic stresses

During the normal operation of the SMES, Electromagnetic forces are induced in the coil following the Lorentz law:

$$\vec{f} = \vec{J} \times \vec{B}$$

Where $\vec{f}$ is the force density, $\vec{J}$ is the current density in the coil and $\vec{B}$ is the magnetic field in the inside the coil. The Figure 19 shows the force density induced in the prototype 0 coil used in the FEM model to calculate the stress in the coil.

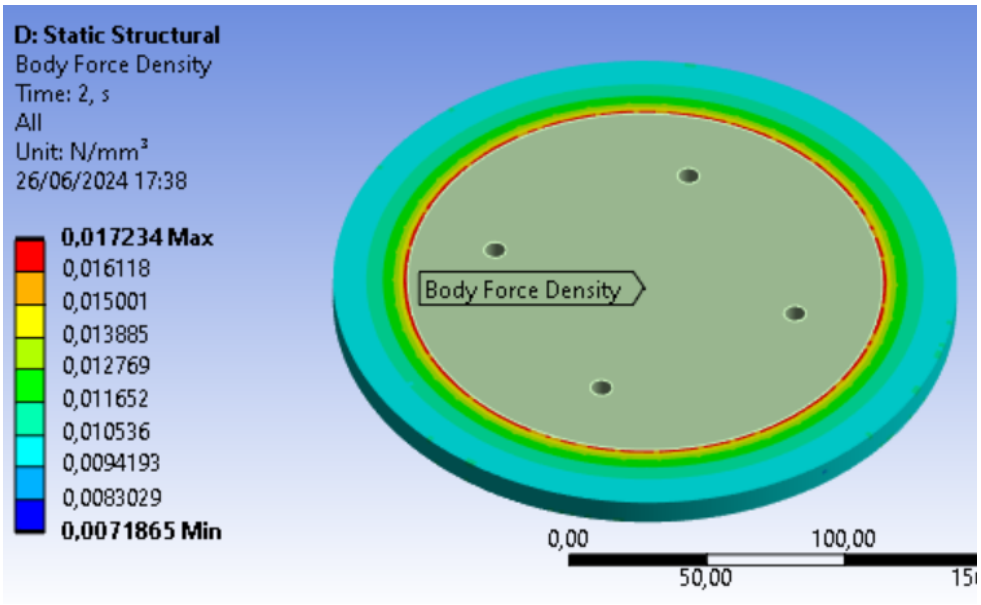

Figure 19: Electromagnetic forces (N/mm³) in prototype 0

To reproduce and evaluate the forces and stresses in the coil, a FEM model was developed. The first step is to simulate the cool down of the coil from room temperature to 77k and evaluate the stresses in the coil due to this cooling process, the second step is to reproduce the nominal operation condition of the coil and evaluate de stress induced by the electromagnetic forces.

Figure 20 and Figure 21 shows the radial and hoop stress in the coil in the FEM model. The model shows that most of the coil has a negative radial stress, that means that most of the coil is working under compression, this compression helps the coil to avoid mechanical degradation and delamination of the different parts of the tape.

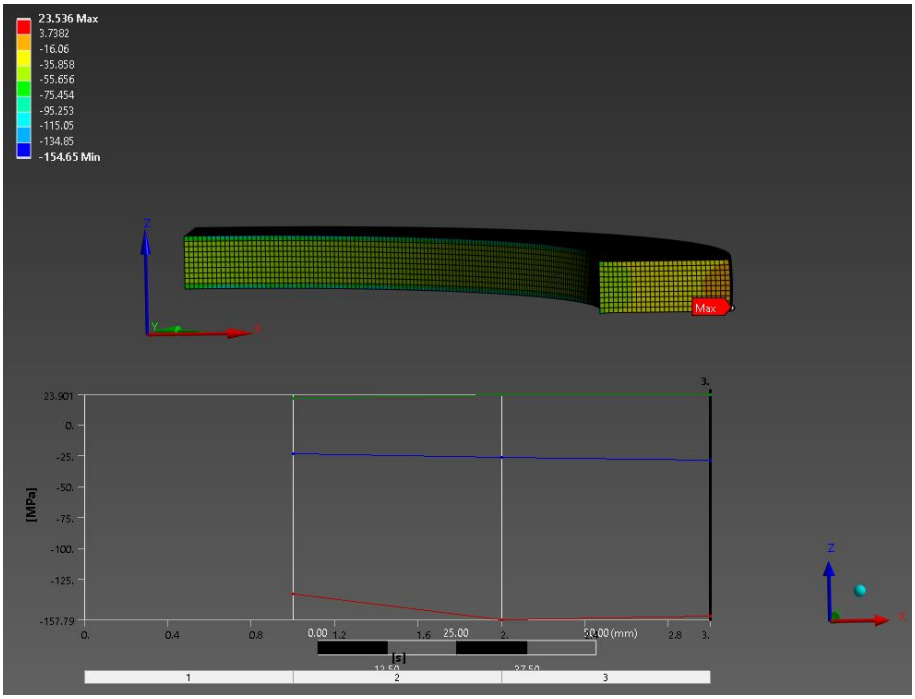

Figure 20: Radial stress in prototype 0

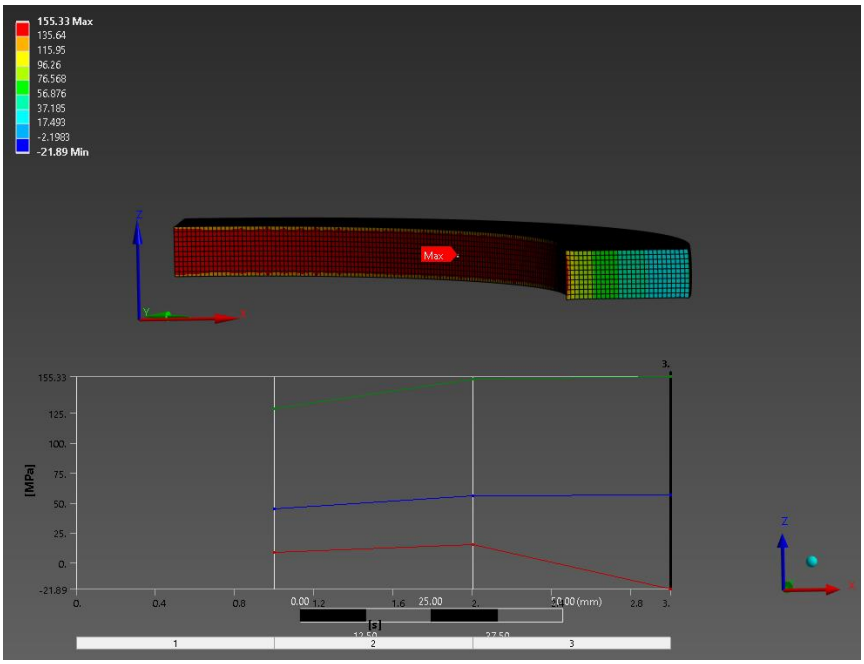

Figure 21: Hoop Stress in prototype 0

4.1.4. PK0-DESIGN SUMMARY

A first prototype was built in the second semester of 2023. The main design variables:

- Ø int: 172 mm.
- Ø ext: 226 mm.
- Number of turns: 82
- Inductance: 9 mH
- Ic (77K) = 69 A.
- Inner mandrel of soft iron.

The coil had the same inner radius as future coils but half the tape length (100m. vs 200m.)

Figure 22 CAS coil (left) V-I curve of CAS prototype for several runs (right)

4.2. TESTING

Several tests were performed to study the characteristic and the behavior of the prototype 0 coil and validate the developed models. First of all, the electromagnetic characteristics, resistance and inductance were measured at room temperature:

Frequency [Hz]	R [Ohm]	L [mH]
DC	2.41	
100	15.44	9.28
120	20.49	9.24
1000	356.16	8.39
10000	2590.00	6.81
100000	15964.00	NAN

4.2.1. LN2 TEST

The coil was tested in an open bath of liquid cryogen of LN2 and LHe. The main objectives of the tests were the measurement of:

- V-I curve
- Resistance of terminal connections
- Strain and stresses

Theoretical V-I curve

Figure 23 shows the theoretical curve and the curve of the tests. The critical current obtained in the various tests is 86 A. This represents a relative error of 24% compared to the theoretical critical current.

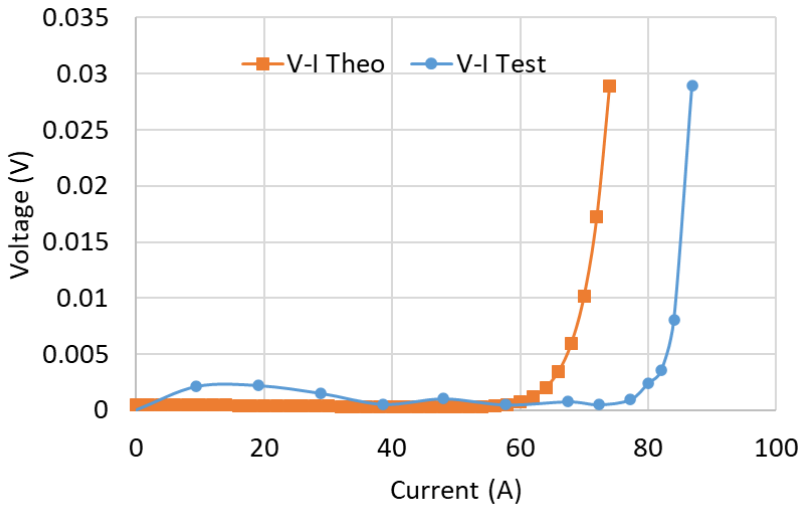

Figure 23: a) Temperature and critical current (under 1uV/cm criterion) for different temperatures; b) Comparison of theoretical and experimental V-I curve at 77K

It is suspected that this discrepancy originates from the difference between the theoretical critical current value of the HTS tape provided by the supplier, which was used for the electromagnetic design, and the actual critical current value obtained once the tape was manufactured, which ended up having an increased performance of 22.9%, making it the most reasonable cause.

Electrical connections

The tests done in LN2 derived a terminal resistance of around 1-5 uOhm.

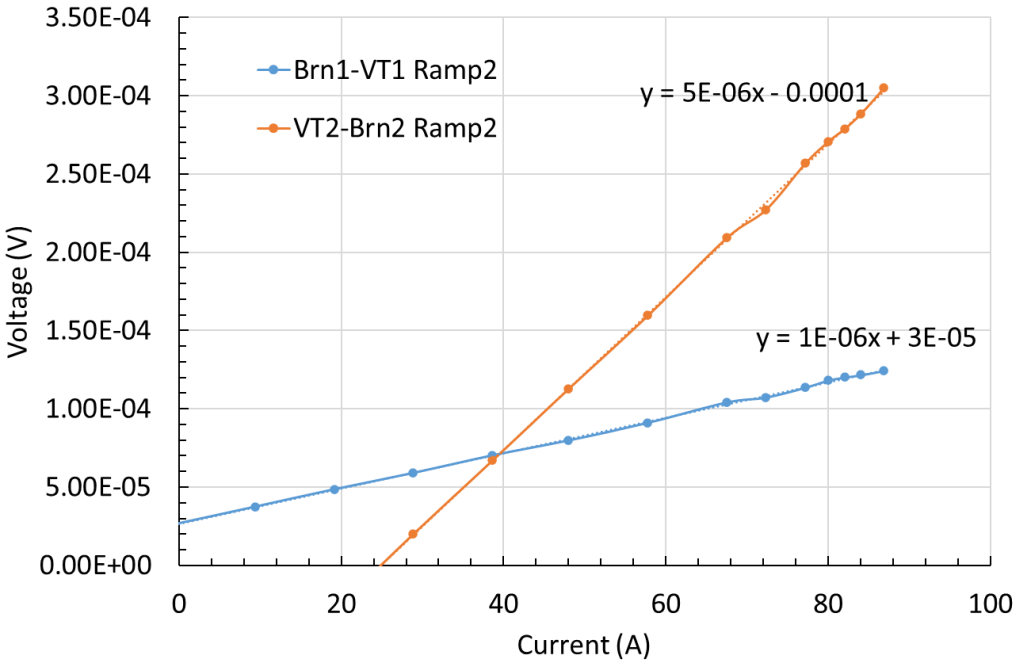

Figure 24 Current (A) vs Voltage drop (V) in electrical connectors

4.2.2. LHE TEST

Current Lead quenches (300A)

In the range of 250-300A the current leads quenched, while the magnet remained superconducting. The quenching of the CL might be explained by the heat generated in the resistive part of the current lead terminals, but it will be checked in the following tests. The CL quench limited the ramp up of the magnet and the measurement of the complete V-I curve. In the next tests, ramps of 50A/s and plateaus of few seconds were performed.

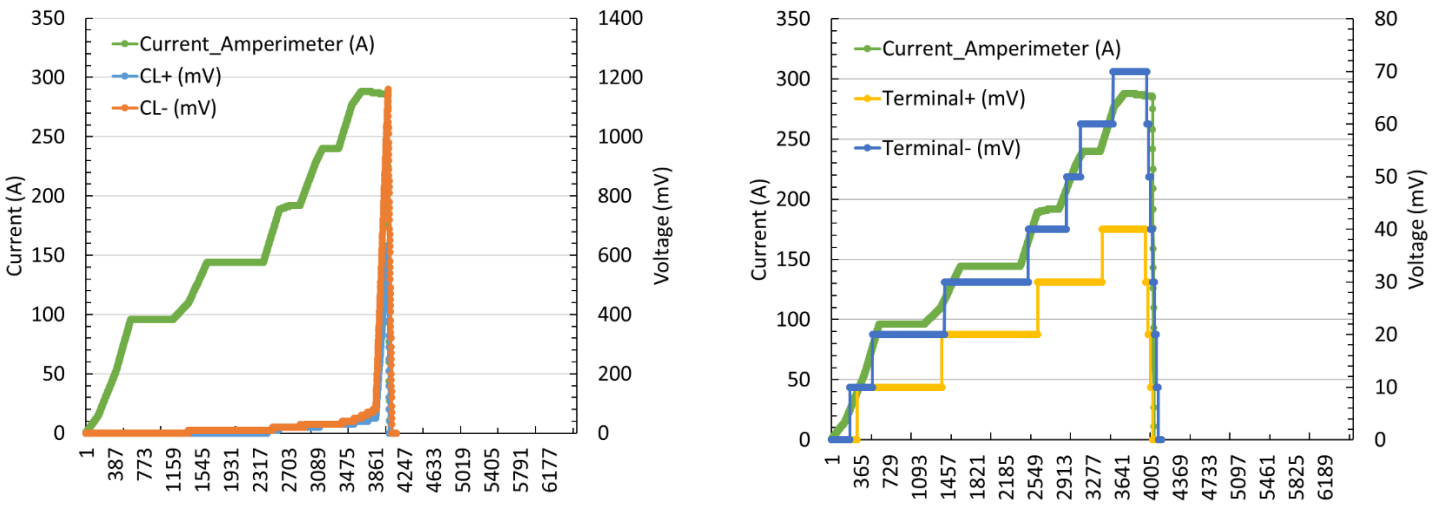

Fig. 2. a) Current lead voltage and b) Voltage in CL terminals, as function of current

Test 500A

The magnet was quickly ramped to 500A, and a "quench" was forced shutting down the system. In this process the most relevant data was acquired with a high-speed acquisition system.

At 500A the magnet remains superconducting with a voltage below the quench voltage criteria (In Fig. 3 the magnet voltage, blue line, is below the quench voltage, grey line)

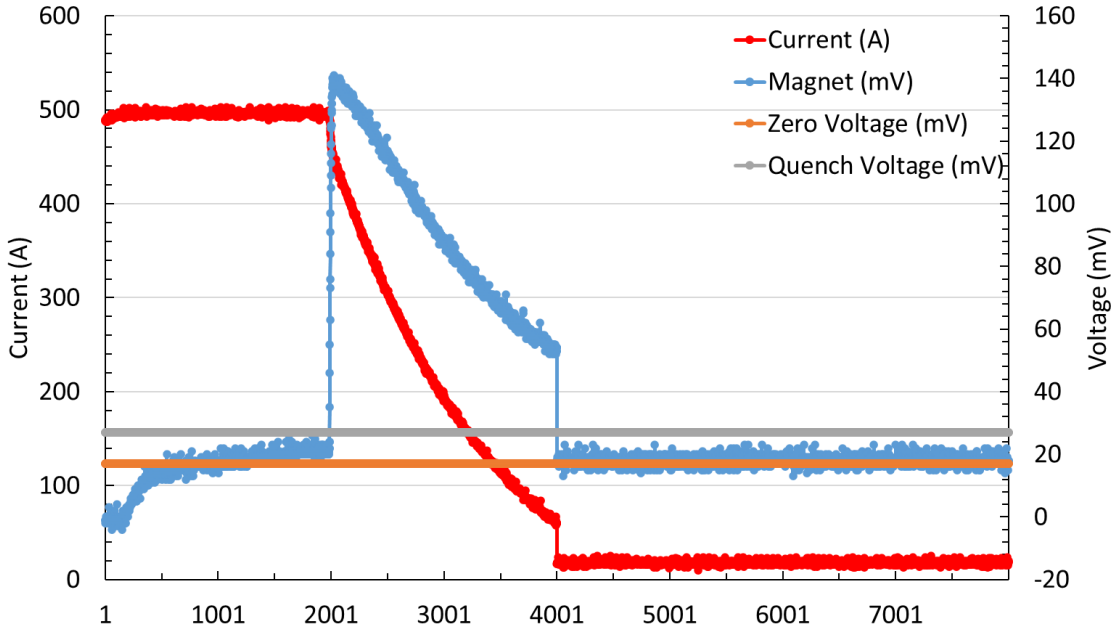

Fig. 3. Current (A) and voltage drop (mV) in the CAS coil at 500A

Test 600A

Same test as before, but the current was increased to 600A. In this case the magnet voltage did surpass the quench voltage limit, however it does not appear to continue developing. More tests are needed to confirm the critical current limit at LHe.

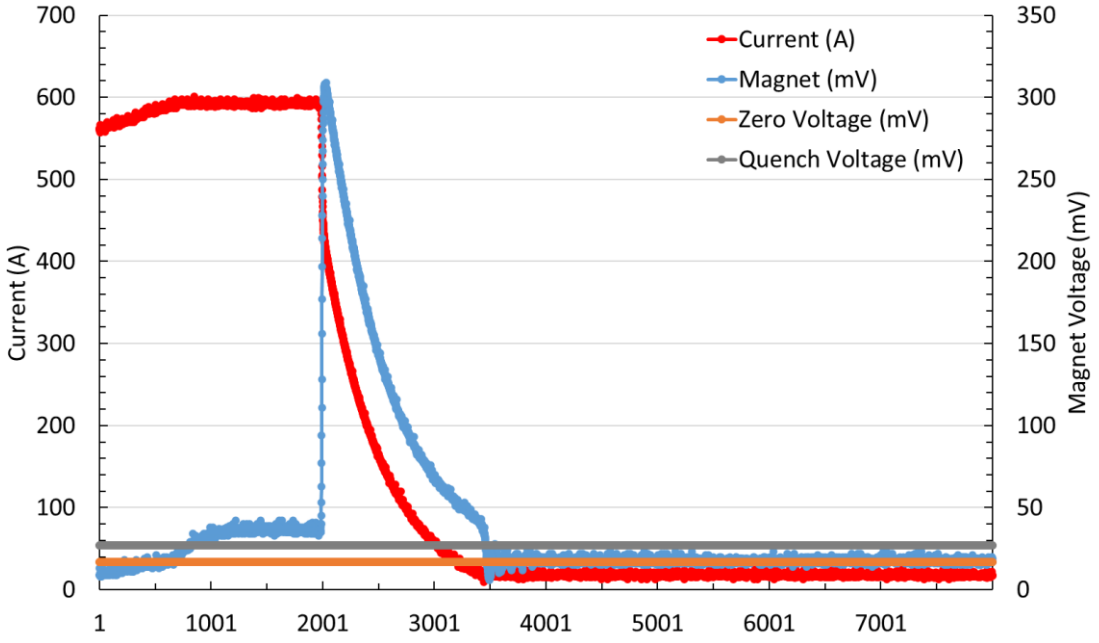

Fig. 4 Current (A) and voltage drop (mV) in the CAS coil at 600A

Electrical connections

Liquid nitrogen – 77K

This time the superconducting current lead was directly soldered to a copper terminal. The resistance is significantly higher this time: 150-250 uOhms (yellow and grey line)

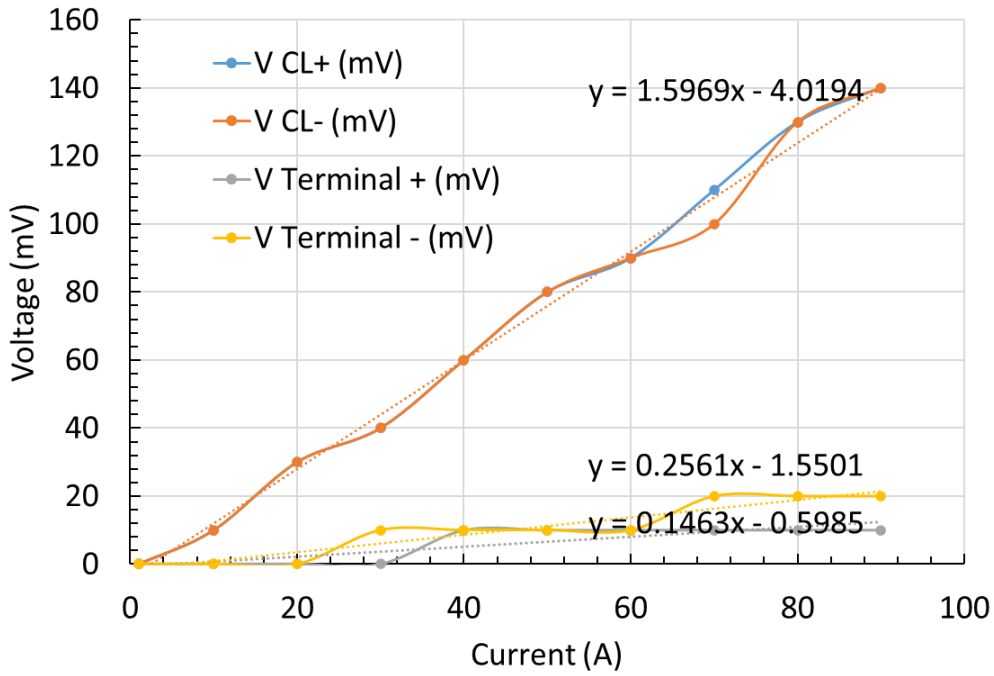

Figure 25 Current (A) vs Voltage drop (V) in electrical connectors at LN2

Liquid helium – 4.2K

At liquid helium the terminal resistance did not decrease, the resistance values were approximately the same: 150-250 uOhms.

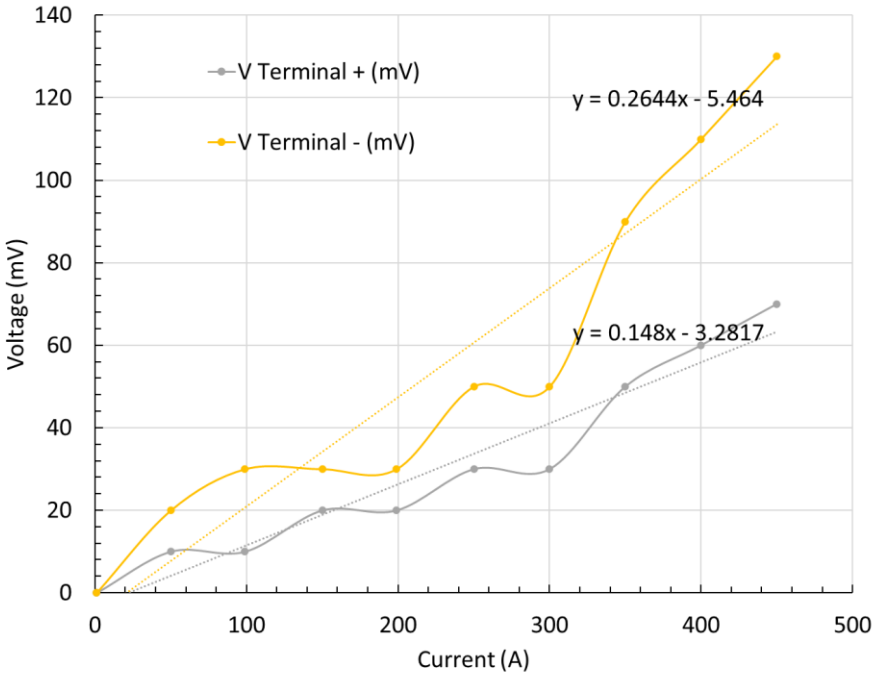

Figure 26 Current (A) vs Voltage drop (V) in electrical connectors at LHe

Lab Setting Comparison

Previous Assembly

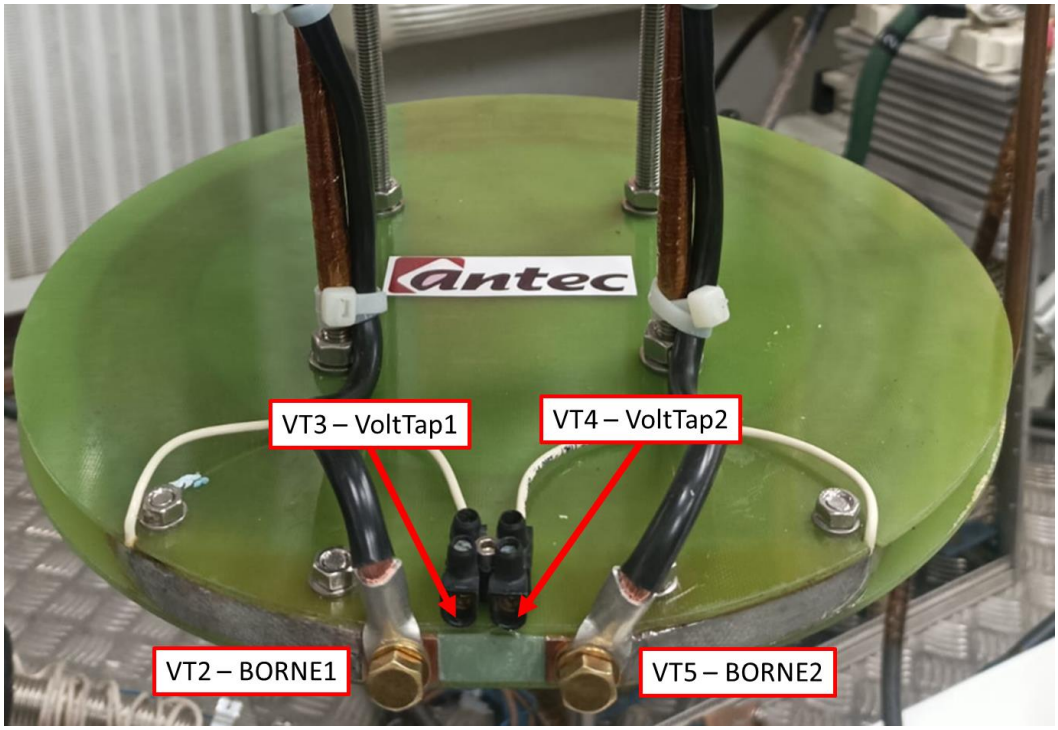

LHe Tests – Assembly

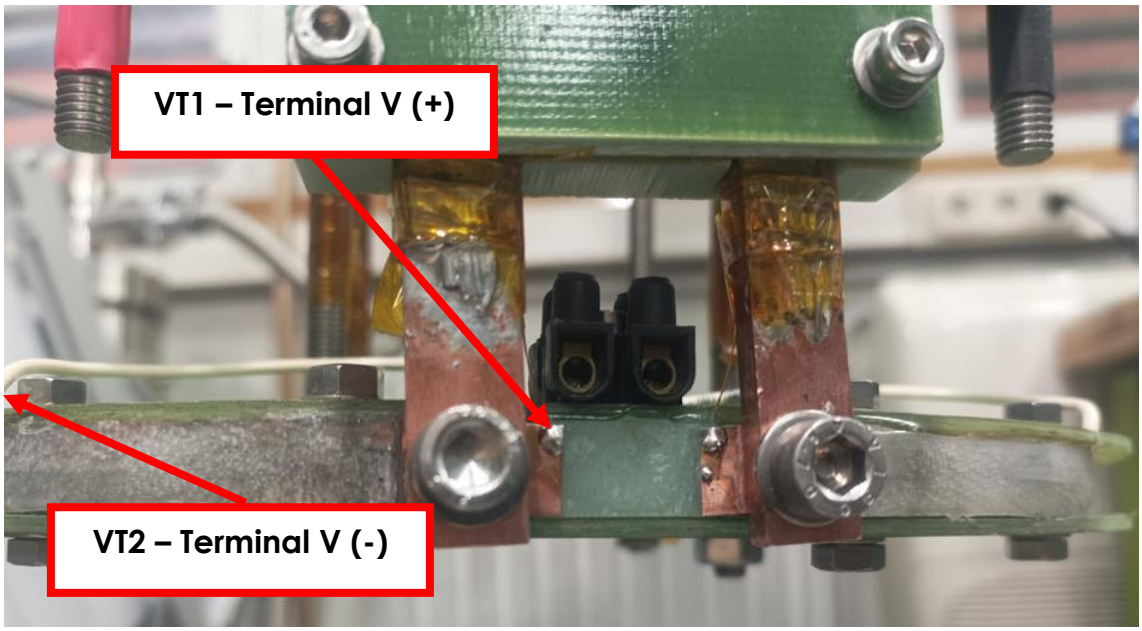

Main Setting Differences

- Current lead contact: In previous tests a copper wire with a traditional terminal was used, and screwed to the magnet terminal. In the LHe test the superconducting CL was soldered to a block of copper. The contact area in the current lead terminal was significantly less.
- Tightening screw: In previous test brass screws were used, and in the LHe test a stainless-steel screw was used.

5. PROTOTYPE 1: PK01

5.1. DESIGN AND FABRICATION

Prototype 1 is the next coil to be manufactured within the POSEIDON framework. There are 2 main objectives: 1) to develop a real module of the POSEIDON SMES, with 200 m. of tape 2) To validate the initial design with experimental testing

5.1.1. ELECTROMAGNETIC DESIGN

The electromagnetic design of prototype 1 will follow the same methodology than the previous coil. The increase in the length of the tape and the change in the material of the inner mandrel of the magnet must be taken into account in the design.

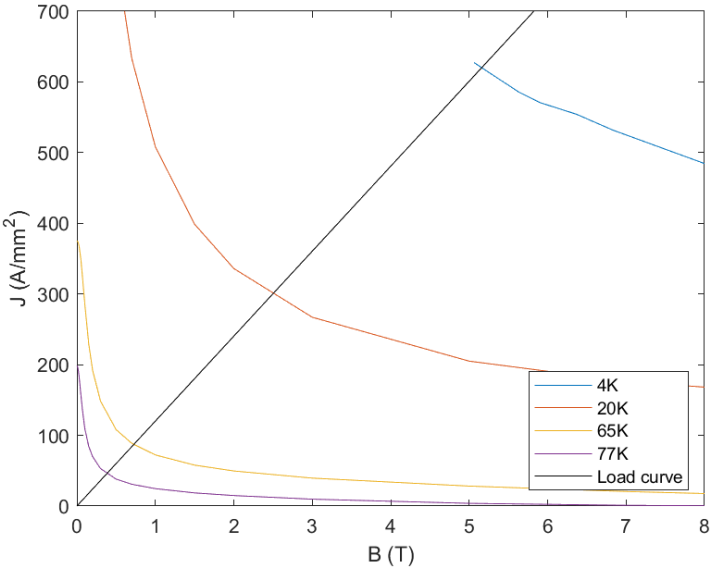

Figure 27: Prototype 1 Load curve

Figure 27 shows the current density vs. magnetic field curves of the coil at different temperatures, and the load curve indicating the critical point at each temperature.

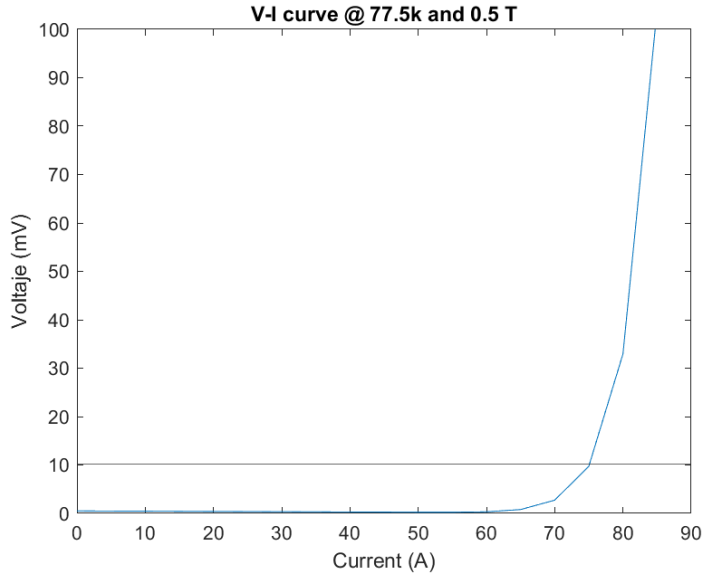

Figure 28: Prototype 1 V-I curve at 77K

In Figure 28 the theorical V-I curve at 77K is shown, the black horizontal line represents the 10 μV/m quench criteria generally used in HTS coils. Table 6 shows the critical current and operation current at different temperatures.

Table 6: Prototype 1 critical currents

Temperature	Critical current (A)	Operation current (A)
77,5 K	75,14	60,11
65 K	141,03	112,83
20 K	486,92	389,54
4,2 K	1002,8	802,21

5.1.2. MECHANICAL DESIGN

After the prototype 0 coil was tested, some mechanical changes were suggested to improve the design in the final POSEIDON coils. The main change in the mechanical design is the modification of the inner mandrel of soft iron by an inner ring of G10.

Several simulations have been performed to evaluate the optimum thickness and material of the new inner ring. In the Figure 29, the results of this study can be seen. Three different materials are studied, stainless steel 316L, isotropic G10 and laminated G10.

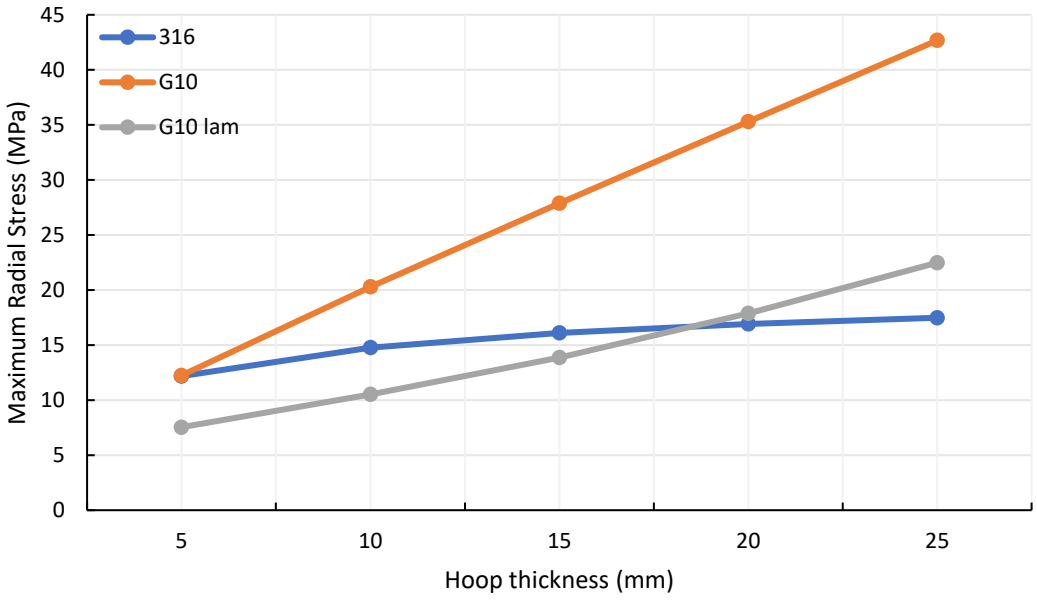

Figure 29:Radial stress as function of hoop thickness for different mandrel materials for PK01 coil

The study shows that the smaller the ring the lower the radial stress in the coil, but for the structural support of the coil a minimum thickness of 10 mm is required. The final design will be with an inner ring of laminated G10 and 10 mm of thickness.

This design has been evaluated with FEM models to validate it. An Ansys FEM model was used to evaluate the stresses during the cooling process up to liquid helium temperatures, 4,2 K, and the electromagnetic forces induced during the normal operation of the SMES.

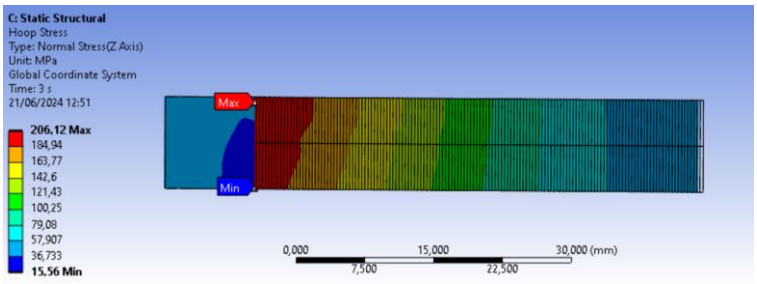

Figure 30: Hoop stress in prototype 1

Figure 30 shows hoop stress in the coil, this is the stress in the azimuthal axis of the coil and is the biggest stress in the coil. This stress must be under the limit, 400 MPa, to avoid the mechanical degradation of the coil.

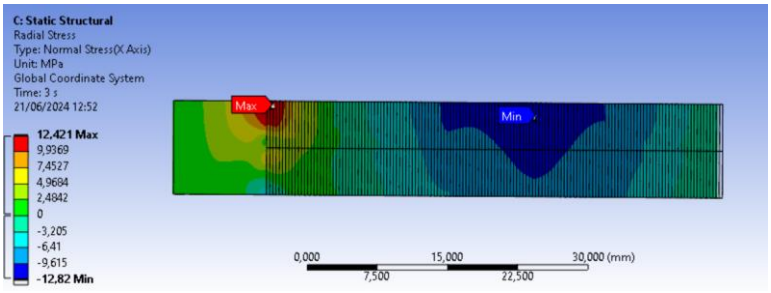

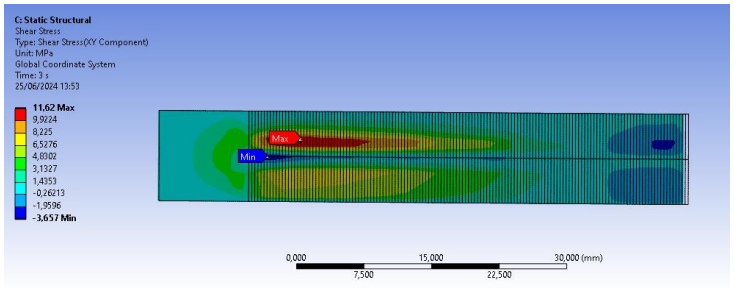

Figure 31: Radial stress and shear stress in prototype 1

Figure 31 shows radial and shear stresses in the coil, these stresses are lower but it's important to keep these stresses low to avoid delamination of the tape.

5.1.3. ELECTRICAL CONNECTIONS

Current leads and electrical joints are an essential part of the design of any superconducting magnet. Current leads aim to electrically connect two points A and B, with the minimum disturbance to the system, i.e. minimum mechanical interference, minimum voltage drop and minimum heat loss. An incorrect dimensioning of the current leads and their connectors can lead to premature quenches such as the ones observed during the liquid helium testing of the PK0.

Schematically a current lead can be divided in two sections:

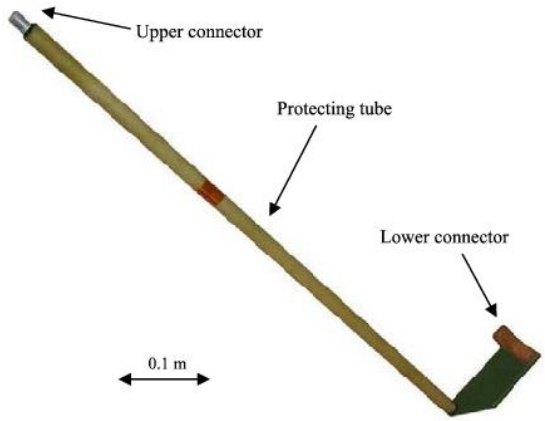

- Connector/Terminal: Connect your current lead to point A/B.
- Straight section: Transport current from point A to point B.

The most important parameter of a current lead is its resistance. The variables that affect the resistance of the two sections of the current lead are:

- Terminal: The contact resistance between point A (or B) and the current lead is non-linear, the main parameters are interdependent with one another:

    - Material
    - Geometry (Contact Area)
    - Contact Pressure
    - Rugosity
    - Material interface
- Straight Section: The resistance of the straight section is more straightforward as it's the product of the material resistivity times its length divided by the cross sections:
    - Material
    - Geometry

A series of experiments are proposed to achieve one main objective: minimize the resistance of a current lead; while having: 1) good mechanical properties 2) robustness 3) Good temperature margin.

To achieve this objective a set of experiments are proposed. The experiment will be divided in two blocks: Experiment 1, focused on the straight section, and Experiment 2, focused on the connector/terminal.

The initial guidelines for the experiments are:

- Experiment 1: Straight Section
    - Reduce resistance → Soldering an HTS tape to a metal section that provides mechanical and electrical support.
    - Mechanical flexibility → Use stranded wires for mechanical support. This gives the possibility of uncoupling the Connector and Straight section.
    - Temperature margin → Use HTS
- Experiment 2: Connectors Section
    - Reduce resistance: Soldering and machining HTS tape + electromechanical support.
    - Temperature margin → Use HTS

Set of experiments 1: Straight Section

The guidelines for the experiments were presented before.

A test specimen, a combination of these variables, is prepared and compared against a virgin specimen.

First experiment consisted of soldering HTS tape to a straight copper section and analyzing: Soldering area, soldering material and soldering flux.

Probe	L	2	Solder	HTS
Probe 1	150	2	SnPb-MBO	Short
Probe 2	150	2	SnPb-MBO	Long
Probe 3	150	2	SnPb-S39	Long
Probe 4	150	2	SnAg-MBO	Short
Probe 5	150	2	SnAg-MBO	Long
Probe 6	150	2	SnAg-S39	Long
Probe 7	150	2		

Sensor nº	Sensor location	I end (A)	V end (mV)	R (uOhm)	P (mW)
V1	Corto-MBO-SnPb	70	0.32	4.57	22.4
V1 HTS		70	0.016	0.23	1.12
V2	Largo-MBO-SnPb	70	0.13	1.86	9.1
V2 HTS		70	0.044	0.63	3.08
V3	Largo-S39-SnPb	70	0.14	2.00	9.8
V3 HTS		70	0.016	0.23	1.12
V4	Corto-MBO-SnAg	70	0.41	5.86	28.7
V4 HTS		70	0.057	0.81	3.99
V5	Largo-MBO-SnAg	70	0.155	2.21	10.85
V5 HTS		70	0.011	0.16	0.77
V6	Largo-S39-SnAg	70	0.081	1.16	5.67
V6 HTS		70	0.048	0.69	3.36
V7		70	0.65	9.29	45.5

The main conclusion from this experiment is that the addition of an HTS tape can decrease the resistance by a factor of almost 10, compare V7 (9.3 Ohms) with V6 (1.16 Ohms). Also, that the tape withstands certain machining as all the long samples provide better results than the short samples.

The second tests consist on soldering an HTS tape to a stranded copper wire and analyze the resistance.

With this solution the parameters involved in the iteration process increases compared to the parameters used for the straight section in the introduction, as we now have a contact resistance at least.

For this solution the main variables that are currently under study are:

- HTS minimum bending radius
- Soldering area
- Soldering material

- Soldering flux

Probe	HTS	D	L	Solder Area	Solder Mat
Probe 1	1	5.5	140	Min A and B	SnAg
Probe 2	0	5.5	140	Min A and B	SnAg
Probe 3	1	9.5	155	Min A and B	SnAg
Probe 4	0	9.5	155	Min A and B	SnAg

Sensor nº	Sensor location	I end (A)	V end (mV)	R (uOhm)	P (mW)
V1		70	0.91	13.00	63.7
V1HTS		70	0.63	9.00	44.1
V2		70	1.07	15.29	74.9
V3		70	0.54	7.71	37.8
V3HTS		70	0.11	1.57	7.7
V4		70	0.58	8.29	40.6

Both HTS probes, probe 1 and 3, show less resistance than the virgin probes. However, the difference is not significant.

The voltage drop in probe 1 is somewhat proportional to the HTS distance relative to the total current lead distance. This appears to indicate that no current is circulating through the HTS tape, it is probably damaged.

However, the voltage drop in the HTS part of probe 3, is not proportional to the HTS-Wire ratio, therefore it appears that the current is in fact flowing through the HTS. The insignificant decrease in resistance is probably due to a large contact resistance. This thesis will be tested in the following runs by increasing the current through the probes.

Set of experiments 2: Connectors

The variables to be studied have been defined, and configurations have been prepared for all possible combinations of variables. For each configuration, the coil was cooled to LN2, a V-I ramp in DC was performed up to 75 Amperes, and then it was heated to change the variable for the next configuration. These were the variables for the test:

- Interface layer: Use of a thin layer of indium in contact areas
- Lateral tightening screw: Stainless steel or brass
- Positive terminal surface: Use one plate on the positive terminal or both plates

Voltage was measured at various points not only to measure the total drop of a terminal but also in segments. This helps to identify which area most of the resistance comes from. Thirteen Voltage Taps were connected at the locations shown in the figure below.

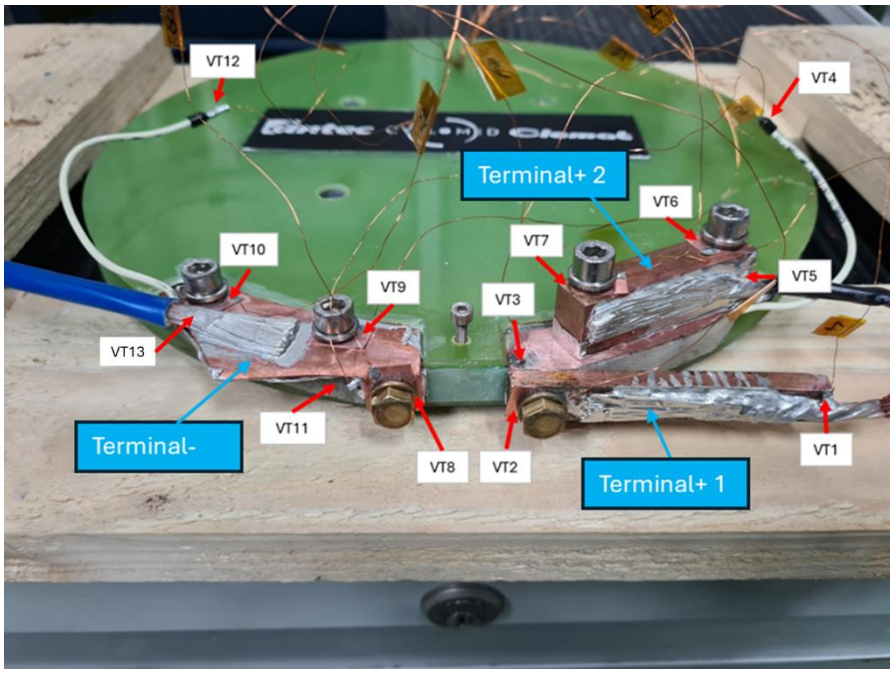

When both positive terminals are connected, the voltage drop of each one is known, but the fraction of current passing through each of them is not, so it is necessary to calculate these two currents to determine the resistance of each terminal.

With 3 variables of 2 options, there are 2^3=8 possible combinations. All combinations were carried out.

The variable *Surface+* is continuous. The contact surface of the different terminals is: *Terminal+1* =117 mm², *Terminal+2* =571 mm², complete positive terminal =688 mm², and *Terminal-* =853 mm².

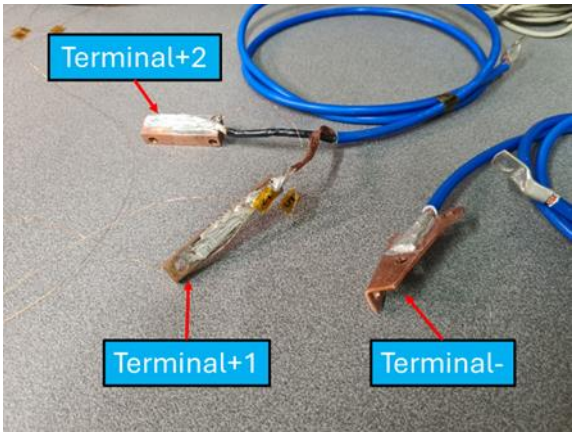

Interface	0: no indium
	1: with indium
Screw	0: stainless steel
	1: brass
Surface+	0: 117 mm²
	1: 688 mm²

The table shows the resistance value of the complete positive and negative terminals. It is worth mentioning that Terminal- was calculated between voltage taps VT12 and VT10.

By performing a statistical analysis of a 2-level factorial design, the values of the regression coefficients in uncoded units of the following terms, both main effects and their interactions, are obtained. The variable *Surface+* being continuous, a value in mm² units is directly introduced, while *Screw* and *Interface* are either 0 or 1.

Configuration				Resistance (μΩ)	
Nº	Interface	Screw	Surface+	Terminal-	Terminal+
1	0	0	0	4.25	15.37
2	0	0	1	3.81	2.99
3	0	1	0	3.64	4.10
4	0	1	1	3.91	1.79
5	1	0	0	0.18	2.61
6	1	0	1	0.04	0.20
7	1	1	0	0.15	2.43
8	1	1	1	0.15	0.23

	Regression coefficients in uncoded units	
Term	Terminal-	Terminal+
Constant	4.030	17.91
Surface+ (A)	-	- 0.02168
Screw (B)	- 0.255	- 13.33
Interface (C)	- 3.920	- 14.80
A*B	-	0.01764
A*C	-	0.01746
B*C	0.295	13.11
A*B*C	-	- 0.01727

Analyzing the obtained results, the following is determined:

- Effect of Area Change:

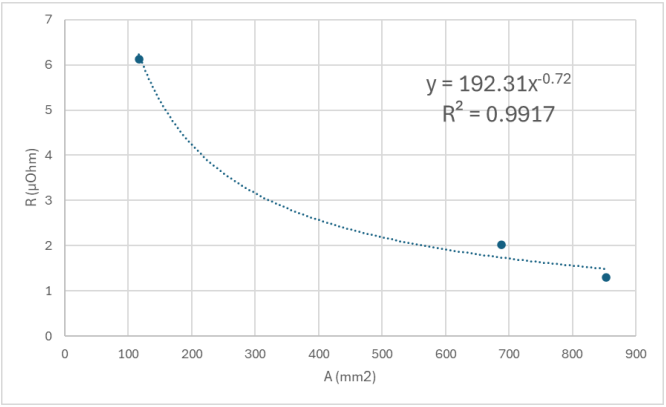

The effect of area change should inversely proportionally affect the surface change. Analyzing the effect within the established domain, it is expected that increasing from 117 to 688 mm² the resistance decreases by 78.71%. The theoretical calculation based on the surface increase gives $100\,(688-117)/688 = 83\%$, closely matching the experimental result with a relative error of 5.17%. Additionally, the resistance value of *Terminal-* fits the resistance vs. surface area curve correctly, obtaining an exponent of b=-0.72, similar to the theoretical value b=-1 expected for an inverse proportional relationship.

- Effect of Interface

Placing an indium interface is expected to decrease resistance by 85%. Due to interaction with the surface variable (as shown below), this value will vary depending on the contact area.

- Effect of Screw

For lateral tightening screws, switching from stainless steel to brass is expected to reduce resistance by 44.31%. Notably, only the lateral screws are changed, while the upper screws of *Terminal+2* are not. This suggests that it is because brass has a similar thermal contraction coefficient to the copper of the terminals, which implies it adapts better in cryogenic temperatures.

- Effect of Interactions

The interactions of the main effects are not negligible as mentioned before. Interaction graphs for *Terminal+* show these interactions according to possible variable options against terminal resistance. If variables had no interaction, the lines would be parallel.

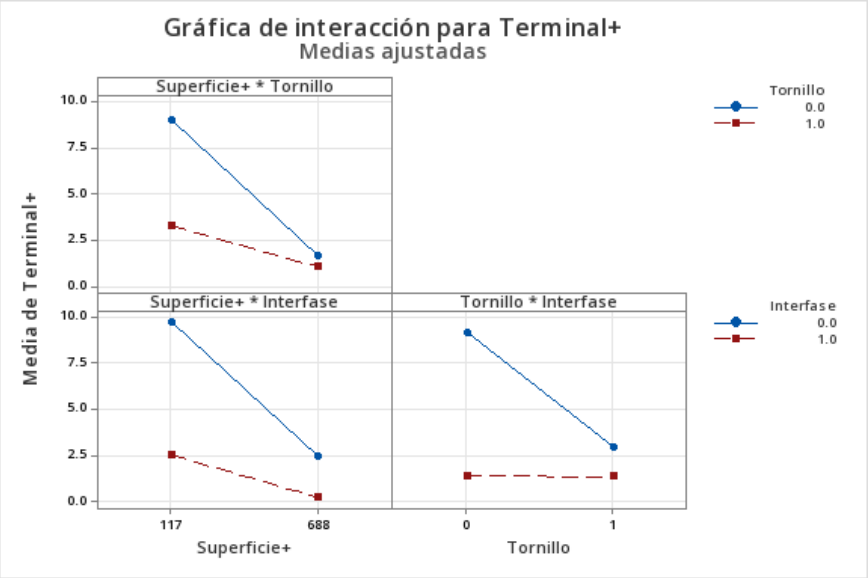

Below are two Pareto charts of the standardized effects on the negative terminal (left) and the effects on the positive terminal (right). The Pareto chart is used to compare and visualize the relative effects of different factors and identify those with the greatest impact. The red line indicating statistical significance appears because the Minitab software requires a confidence interval for this graph, but it does not apply to this analysis, which only compares relative effects.

It has been observed that most of the voltage drop of *Terminal+1* comes from the VT1-VT2 section, which is the section between the positive current lead and the copper plate

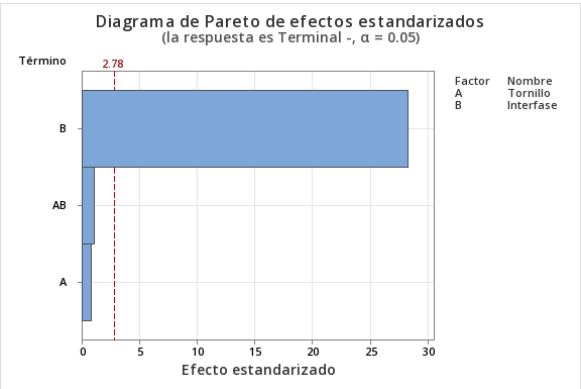

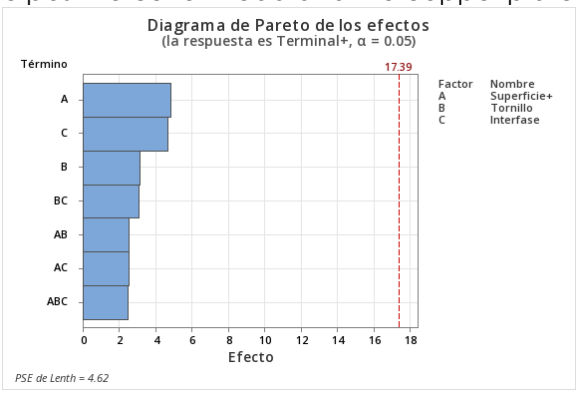

to which this cable is soldered, suggesting that this drop comes from the solder resistance.

5.1.4. P1-DESIGN SUMMARY

<u>Prototype 1:</u> Geometric parameters

- Ø int: 172 mm.
- Ø ext: 270 mm.
- Number of turns: 144
- Tape length: 200 m.

5.2. NEXT STEPS: MANUFACTURING AND TESTING

All parts of PK01 coil have been designed and validated, including the development of the manufacturing drawings which are included as an annex. Currently all parts are being manufactured and is expected that the PK01 will be ready for testing in the weeks following the submission of this report.

In these tests the design process and models will be validated, including:

1) Electromagnetic design: measurement of V-I curve, measurement of magnetic field.
2) Mechanical design: measurement of strains in the coil.
3) Cooling system: measurement in AC in equivalent SMES operation

6. SMES MAGNET

6.1. SUPERCONDUCTING MAGNET

The final SMES superconducting magnet will be composed of 12 double pancake coils stacked to form a solenoid magnet, Figure 32 shows the current CAD model. The solenoidal design is based on the modularity and adaptability of the single double pancake coil. The number of pancakes can be increased if the energy of the SMES needs to be increased.

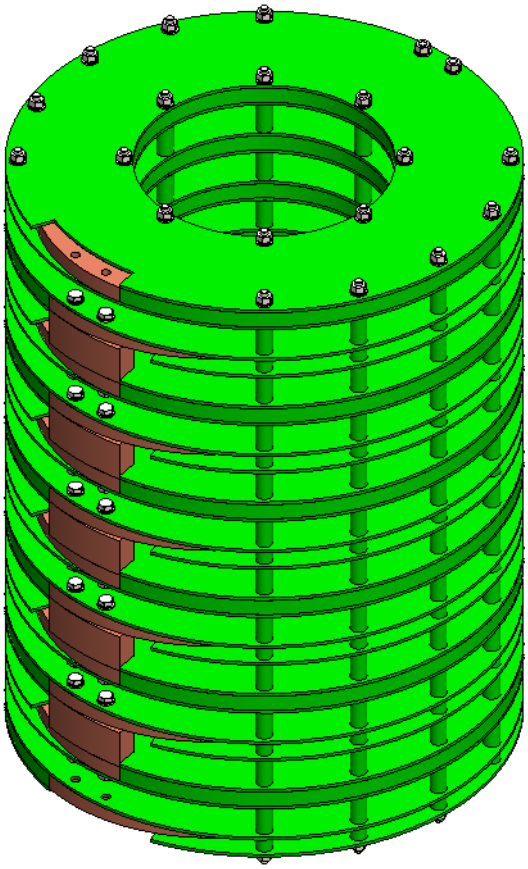

Figure 32: CAD of the superconducting magnet

The electromagnetic properties of a magnet are determined by the geometry and the characteristics of the HTS material. In particular, in the HTS tapes, screening currents appear to expel the magnetic field from the interior of the tape. The screening currents in the magnet must be evaluated due to the large forces induced in the coil, Figure 33. This forces have been taken into account in the design of PK01.

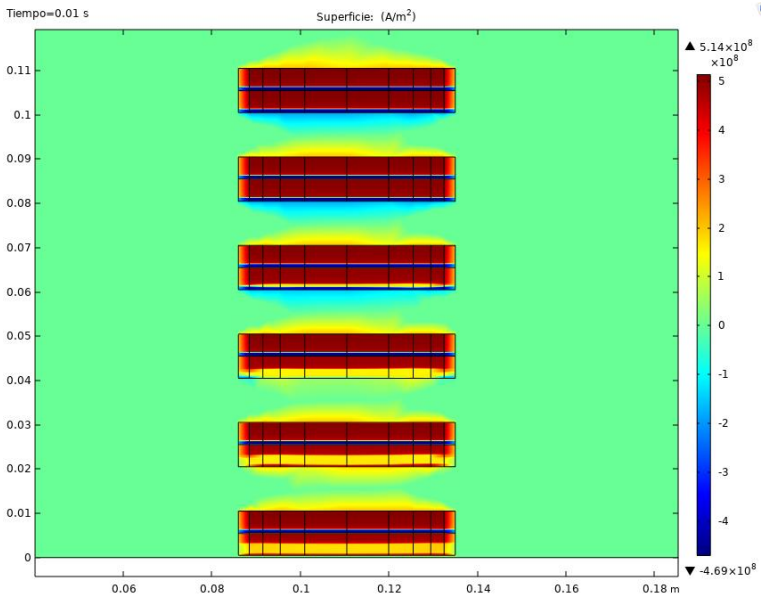

Figure 33: Electromagnetic model of the SMES magnet

6.2. CRYOGENIC SYSTEM

The proposed cryogenic system in the conceptual design is maintained, which was based on the use of a cryogenic supply system, which circulates Helium temperature from ambient temperature to cryogenic temperature with the aid of a cryocooler. However, the design for manufacturing of this system is postponed as one of the limitations is that it must be designed ad-hoc, and any change from the initial parameters would require a design modification. Therefore, to allow for quick iteration between design and experiment, more traditional cryogenic systems are preferred in the early stage of development, i.e. the use of open cooling systems such as cryostats with liquid cryogen (Liquid Nitrogen 77K, and Liquid Helium at 4.2K). The final design and the manufacturing drawings of the cryogenic system will be included in the next deliverable.

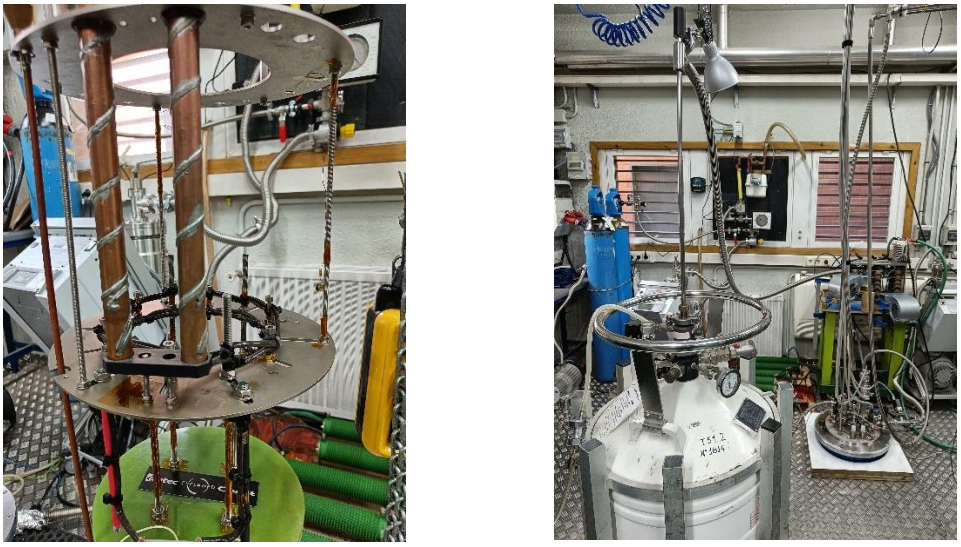

Figure 34 PK0 coil being tested ina cryostat in CIEMAT facilities (left) and picture during LHe testing of PK0 coil (right)

However, not all tests are being done in open systems, currently PK0 is being prepared to be tested in a cooling conduction scheme, which is a potential long term solution. This

test will allow us to measure the robustness of the coil to several cooling cycles, to characterize the coil behavior at different temperatures, and to detect hot spots in the coil.

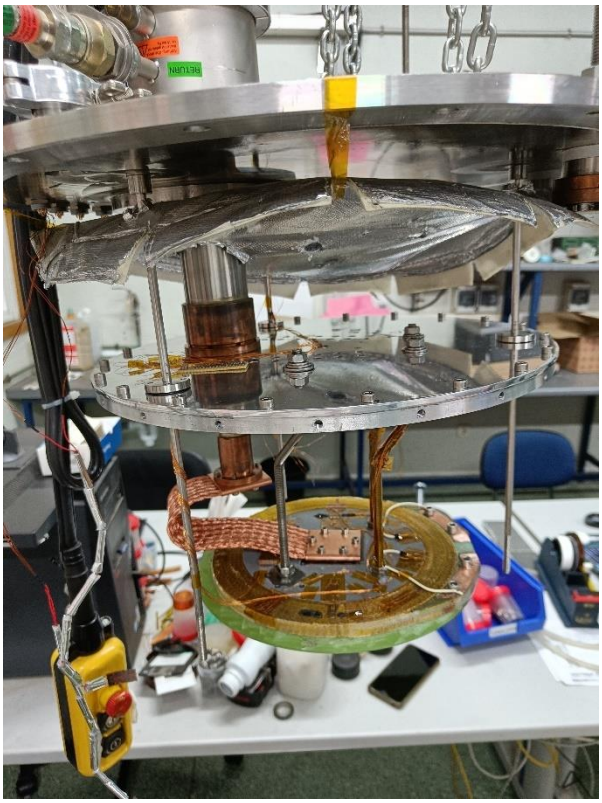

Figure 35 PK0 coil being tested in a 2-stage Gifford-McMahon cryocooler

Next step, which will start in the followings weeks, after the LHe testing of PK01, will be the design and testing of the flow refrigeration configuration. The final design and configuration will be presented in the following deliverables.

6.3. POWER CONVERTER

The selected power converter was a simplified version of the VSC in which we use a commercial bipolar power supply connected to the grid and a chopper with flywheel diodes and a load to recover the stored energy in the coil.

The commercial power source has already been tested and a control system has been developed for the correct operation of the SMES.

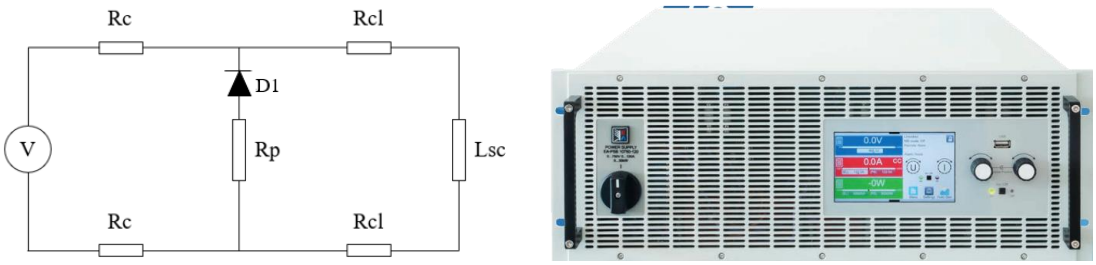

Figure 36. Schematic of the electrical circuit of the experimental test at LHe of the PK0 coil and commercial power source used in the tests.

7. CONCLUSIONS

The SMES system developed in the POSEIDON project shows potential for marine power systems, especially for ships with high-duty cycles (e.g., short river ferries). Conventional Li-ion batteries struggle to meet these demands, but SMES offers a high specific power solution that can improve energy management.

The use of high-temperature superconductors (HTS), specifically 2G HTS tape from Shanghai Superconductors, represents a significant choice due to its high critical temperature, which reduces cooling energy costs. The solenoidal design of the magnet with double-pancake coils also ensures scalability and ease of fabrication, providing a modular design that can be adapted based on energy requirements.

The document addresses several challenges in HTS technology, including mechanical degradation, AC losses, and current lead performance. These have been partly mitigated through advanced modeling, early prototyping (e.g., PK0 and PK01), and specific design choices. However, challenges like screening currents and low quench propagation velocity in HTS magnets remain. To reduce and mitigate the risk a more aggressive prototyping and testing iterative development has been adopted.

Testing and Iterative Development: Testing has been a critical aspect of validating the designs. Prototype 0 testing highlighted discrepancies between theoretical and actual critical current values, due to suppliers variability. For Prototype 1 (PK01), the design was modified to include an improved mechanical design (e.g., a G10 inner ring) to mitigate mechanical stress.

Power and Control System: The chosen power converter system uses a Voltage Source Converter (VSC) with a commercial bipolar power supply. This setup allows for independent control of active and reactive power while maintaining a low Total Harmonic Distortion (THD). This design is well-suited for integrating SMES into marine electrical systems.

Future Work and Scalability: The document outlines plans for further prototyping and testing, particularly with the SMES's integration into more advanced cryogenic systems and improving the electrical connections in superconducting coils. The modular nature of the system allows for scaling up to meet larger energy demands in the future.

8. BIBLIOGRAPHY

[1] H. Maeda and Y. Yanagisawa, "Recent Developments in High-Temperature Superconducting Magnet Technology (Review)," *IEEE Trans. Appl. Supercond.*, vol. 24, no. 3, Jun. 2014, doi: 10.1109/TASC.2013.2287707.

[2] J. Xia, H. Bai, H. Yong, H. W. Weijers, T. A. Painter, and M. D. Bird, "Stress and strain analysis of a REBCO high field coil based on the distribution of shielding current," *Supercond. Sci. Technol.*, vol. 32, no. 9, p. 095005, Jul. 2019, doi: 10.1088/1361-6668/AB279C.

9. ANNEX

9.1. PK0

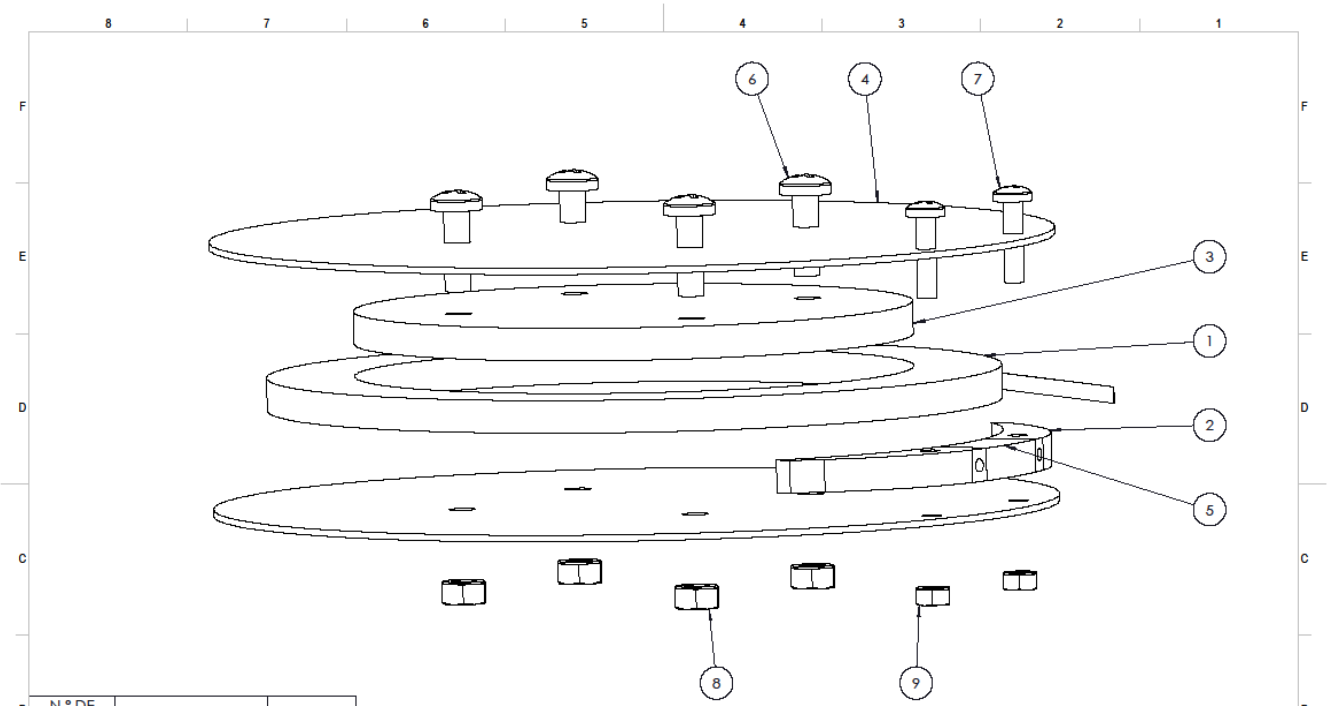

N.º DE ELEMENTO	N.º DE PIEZA	CANTIDAD
1	Pancake_86mm	1
2	DP_Conector_86mm	2
3	Mandrino_Hierro	1
4	Tapa_hierro	2
5	Separador_G11	1
6	Tornillo M8	4
7	Tornillo M6	2
8	ISO - 4032 - M8 - W - N	4
9	ISO - 4032 - M6 - W - N	2

Material:	Acabado:	Peso (g):	Definición de estados superficiales según UNE-EN ISO 1302, 4287 Y 4288. Principio de tolerancias fundamentales según ISO 8015 (UNE 1-149-90. Desviaciones admisibles según UNE-EN 22768. Clase de tolerancia mK.
Tratamiento:	Formato: A3 / Cantidad: 1 / Escala: 1:1		Conjunto: / Hoja: 1/1
	Nombre:	Fecha:	Subconjunto:
	Proyectado: C.Gil	22/08/23	Denominación: Bobina CAS
	Verificado: C. Hernando	22/08/23	Sustituye a: / Sustituido por:
Restricciones de uso del documento, según ISO 16016	ISO 13715		Plano Nº: / Rev.: 1

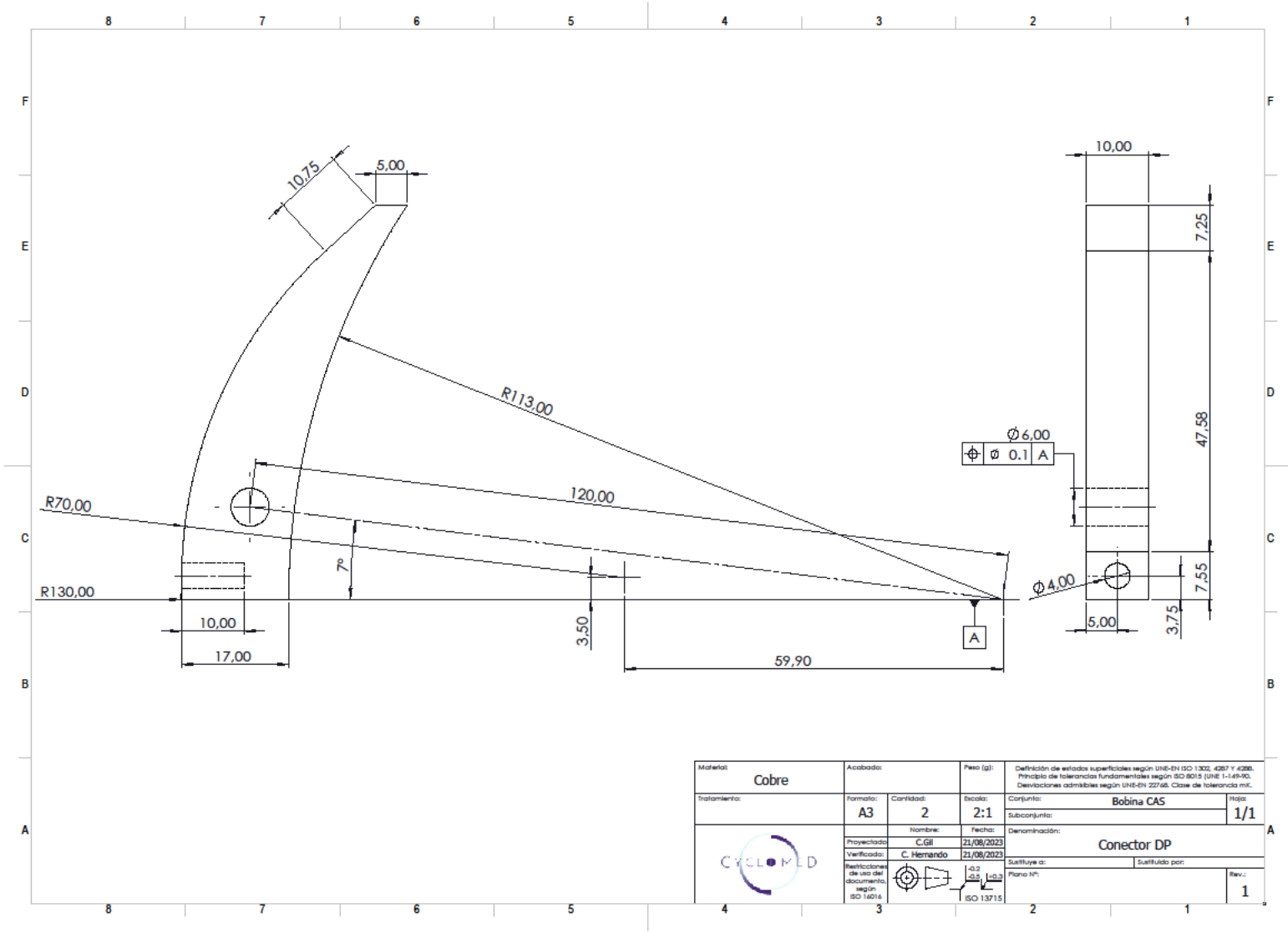
10,75
5,00
R113,00
120,00
R70,00
R130,00
7
10,00
17,00
3,50
59,90
A
10,00
7,25
47,58
Ø6,00
Ø 0.1 A
Ø4,00
7,55
3,75
5,00
Material: Cobre
Tratamiento:
Acabado:
Peso (g):
Formato: A3
Cantidad: 2
Escala: 2:1
Hoja: 1/1
Conjunto: Bobina CAS
Subconjunto:
Denominación: Conector DP
Nombre:
Fecha:
Proyectado: C.Gil 21/08/2023
Verificado: C. Hernando 21/08/2023
Sustituye a:
Sustituido por:
Plano Nº:
Rev.: 1
ISO 13715

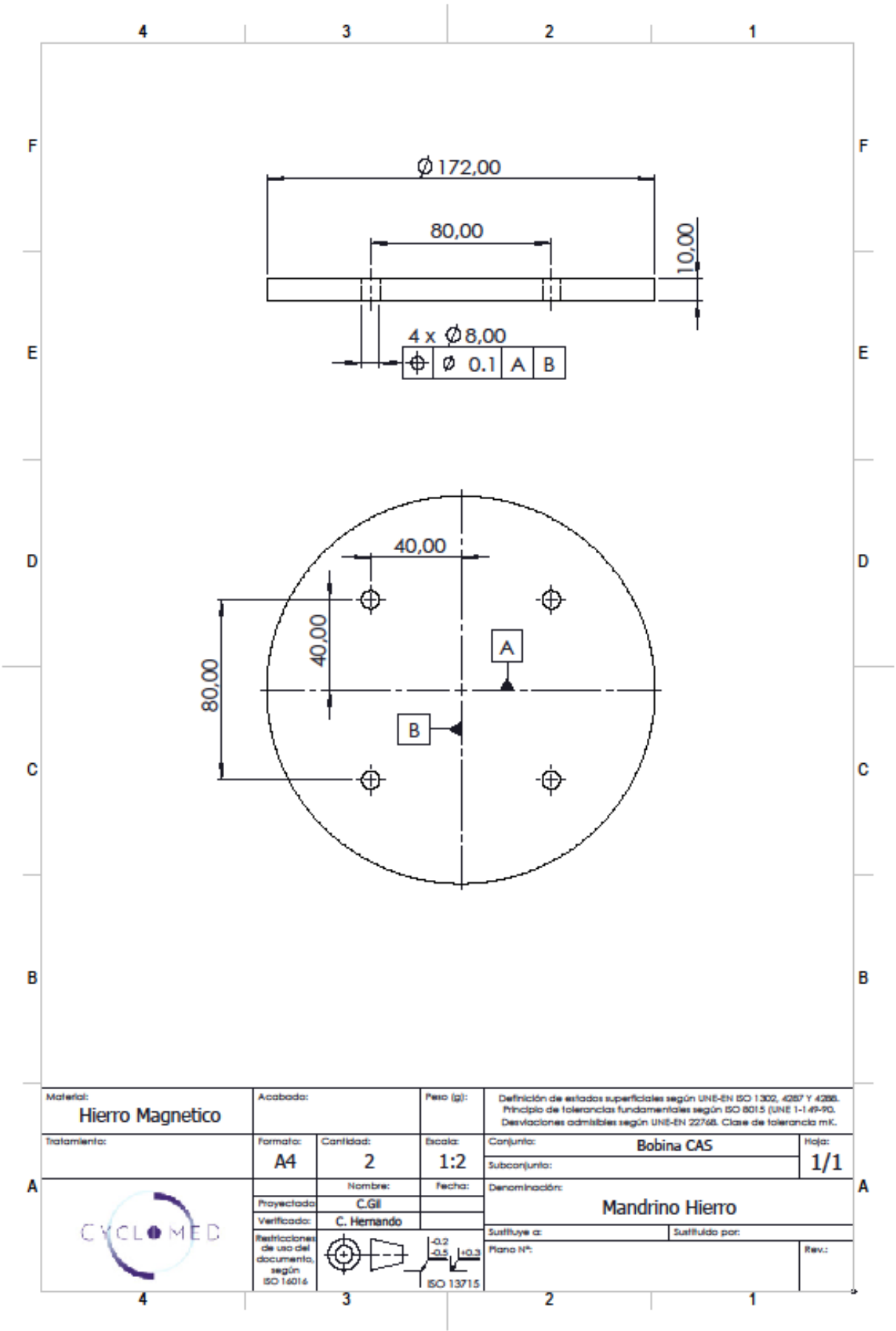
Ø 172,00
80,00
10,00
4 x Ø 8,00
Ø 0.1 A B
40,00
40,00
80,00
A
B
Material:
Hierro Magnetico
Acabado:
Peso (g):
Definición de estados superficiales según UNE-EN ISO 1302, 4287 Y 4288.
Principio de tolerancias fundamentales según ISO 8015 (UNE 1-149-90.
Desviaciones admisibles según UNE-EN 22768. Clase de tolerancia mK.
Tratamiento:
Formato:
A4
Cantidad:
2
Escala:
1:2
Conjunto:
Bobina CAS
Hoja:
1/1
Subconjunto:
Nombre:
Fecha:
Denominación:
Mandrino Hierro
Proyectado:
C.Gil
Verificado:
C. Hernando
Sustituye a:
Sustituido por:
Restricciones de uso del documento, según ISO 16016
ISO 13715
Plano Nº:
Rev.:
CYCLOMED

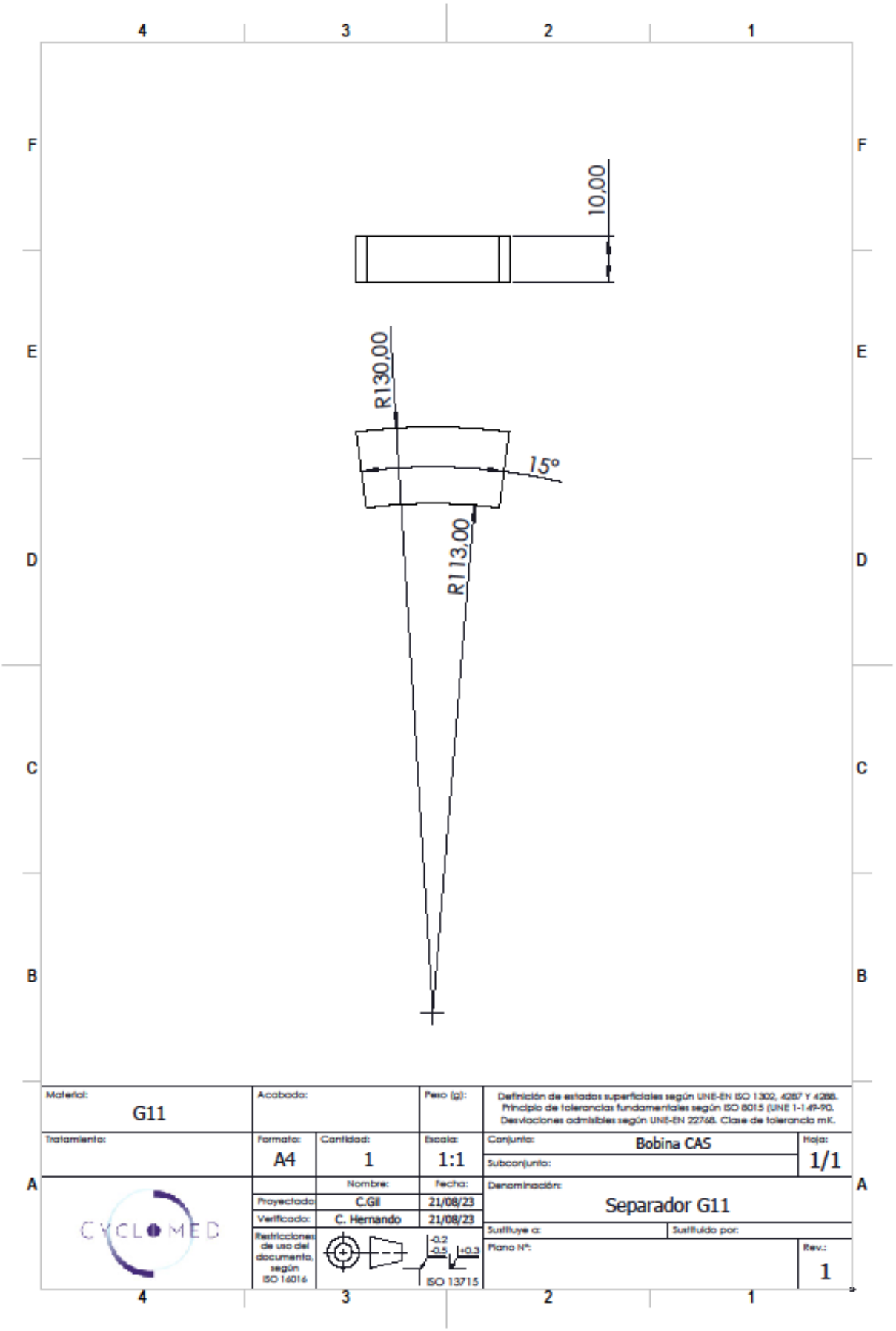

Material: G11	Acabado:		Peso (g):	Definición de estados superficiales según UNE-EN ISO 1302, 4287 Y 4288. Principio de tolerancias fundamentales según ISO 8015 (UNE 1-149-90. Desviaciones admisibles según UNE-EN 22768. Clase de tolerancia mK.	
Tratamiento:	Formato: A4	Cantidad: 1	Escala: 1:1	Conjunto: Bobina CAS	Hoja: 1/1
				Subconjunto:	
CYCLOMED		Nombre:	Fecha:	Denominación: Separador G11	
	Proyectado	C.Gil	21/08/23		
	Verificado:	C. Hernando	21/08/23		
	Restricciones de uso del documento, según ISO 16016		ISO 13715	Sustituye a:	Sustituido por:
				Plano Nº:	Rev.: 1

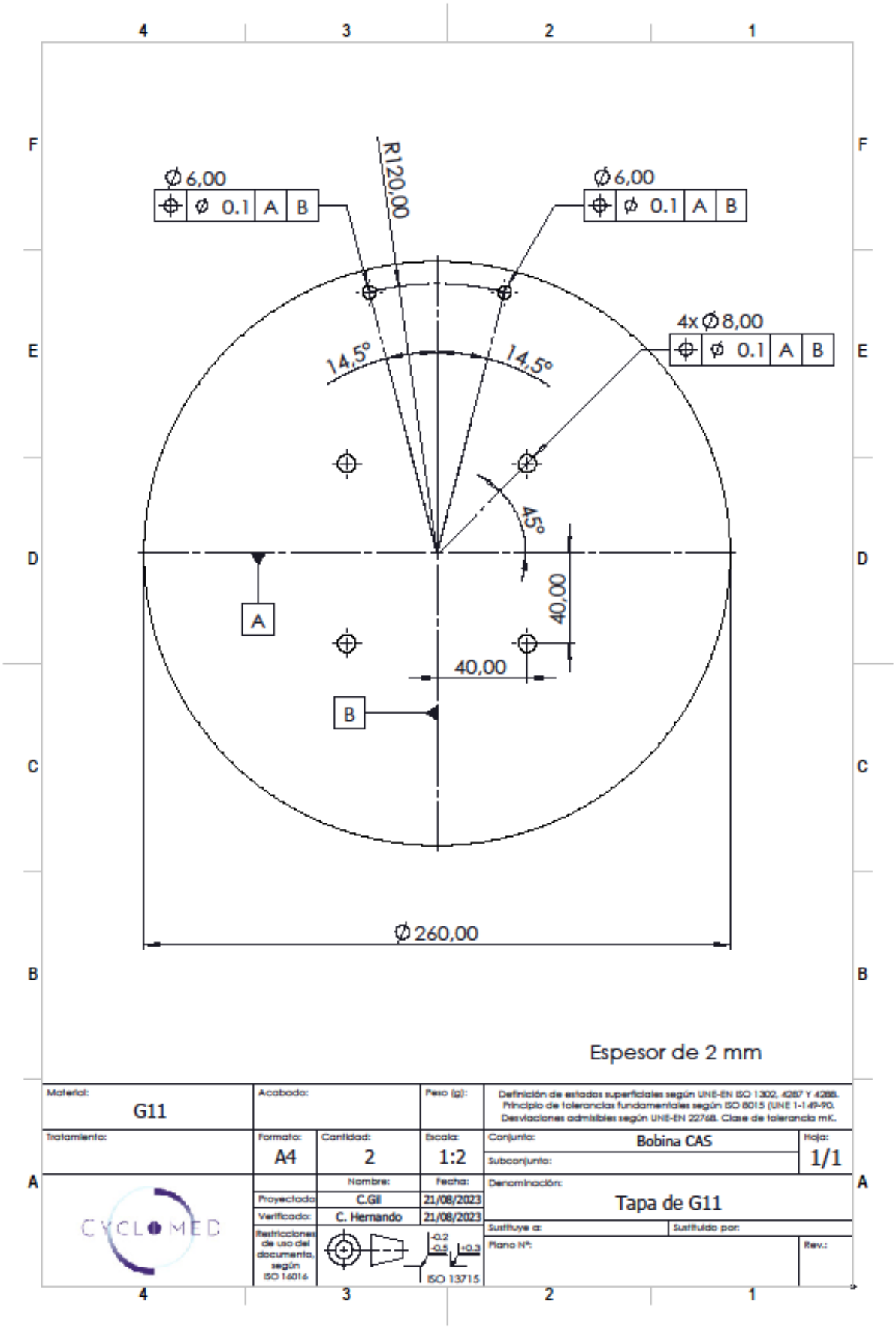
Ø6,00
Ø 0.1 A B
R120,00
Ø6,00
Ø 0.1 A B
4xØ8,00
Ø 0.1 A B
14,5°
14,5°
45°
40,00
40,00
A
B
Ø260,00
Espesor de 2 mm
Material: G11
Acabado:
Peso (g):
Definición de estados superficiales según UNE-EN ISO 1302, 4287 Y 4288. Principio de tolerancias fundamentales según ISO 8015 (UNE 1-149-90. Desviaciones admisibles según UNE-EN 22768. Clase de tolerancia mK.
Tratamiento:
Formato: A4
Cantidad: 2
Escala: 1:2
Conjunto: Bobina CAS
Hoja: 1/1
Subconjunto:
Nombre:
Fecha:
Proyectado C.Gil 21/08/2023
Verificado: C. Hernando 21/08/2023
Denominación: Tapa de G11
Restricciones de uso del documento, según ISO 16016
ISO 13715
Sustituye a:
Sustituida por:
Plano Nº:
Rev.:
CYCLOMED

9.2. PK01

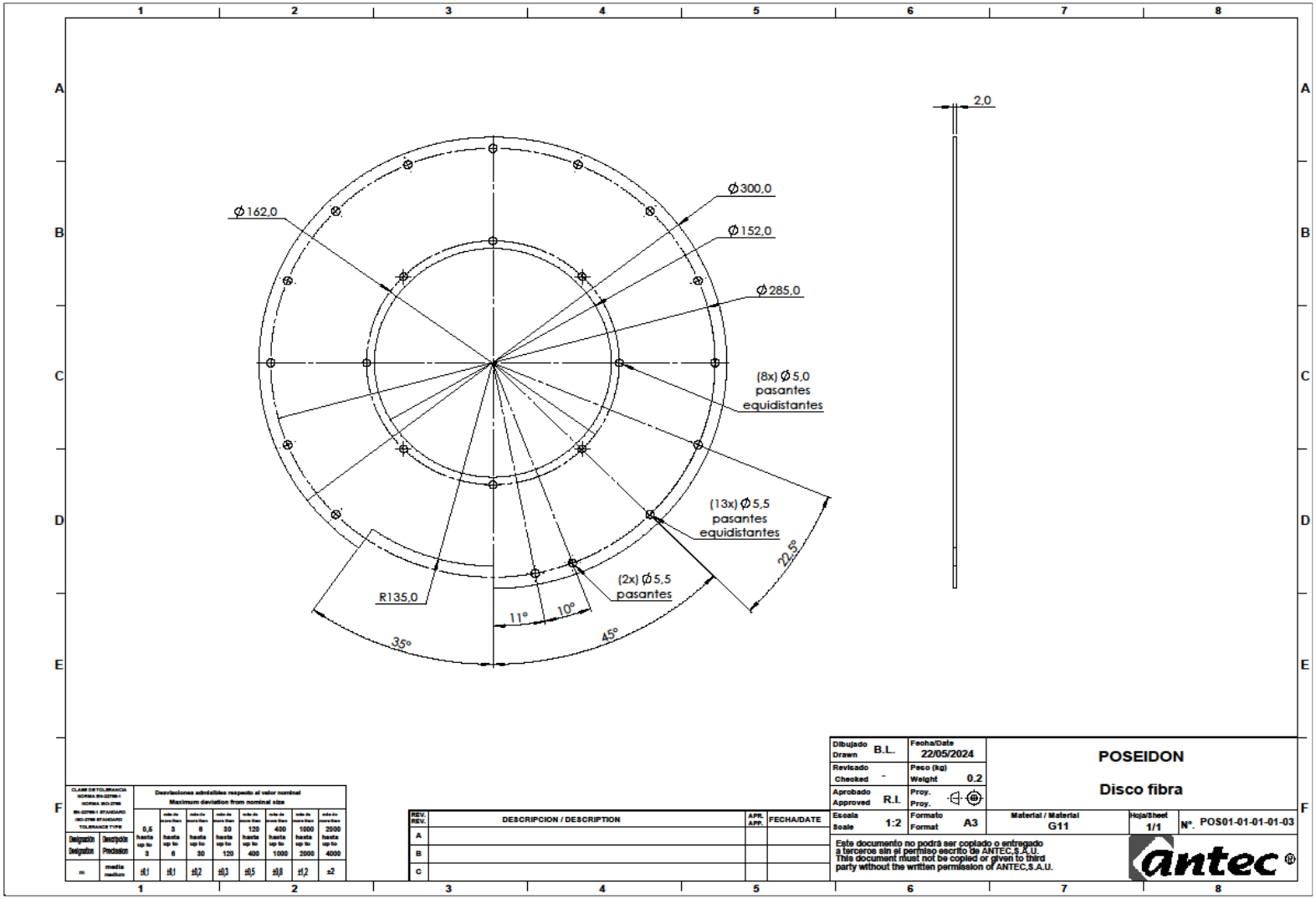
2,0
Ø300,0
Ø162,0
Ø152,0
Ø285,0
(8x) Ø5,0
pasantes
equidistantes
(13x) Ø5,5
pasantes
equidistantes
22,5°
(2x) Ø5,5
pasantes
R135,0
11°
10°
45°
35°
Dibujado Drawn B.L.
Fecha/Date 22/05/2024
Revisado Checked -
Peso (kg) Weight 0.2
Aprobado Approved R.I.
Proy. Proy.
Escala Scale 1:2
Formato Format A3
POSEIDON
Disco fibra
Material / Material G11
Hoja/Sheet 1/1
Nº. POS01-01-01-01-03
Este documento no podrá ser copiado o entregado a terceros sin el permiso escrito de ANTEC,S.A.U.
This document must not be copied or given to third party without the written permission of ANTEC,S.A.U.
antec
REV. REV.
DESCRIPCION / DESCRIPTION
APR. APP.
FECHA/DATE
A
B
C

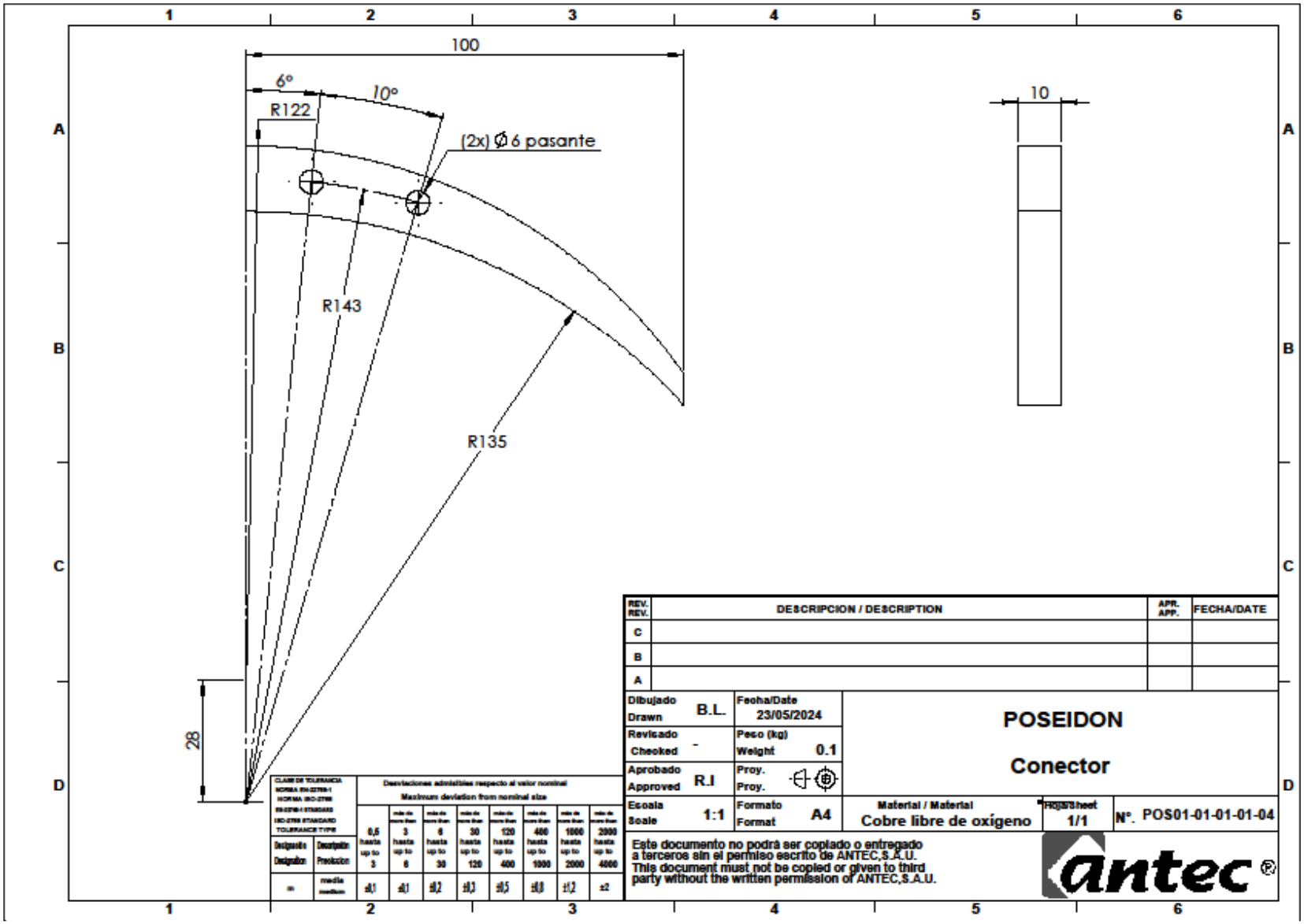
100
6°
10°
R122
(2x) Ø 6 pasante
R143
R135
28
10
DESCRIPCION / DESCRIPTION
FECHA/DATE
Dibujado / Drawn B.L.
Fecha/Date 23/05/2024
Revisado / Checked -
Peso (kg) / Weight 0.1
Aprobado / Approved R.I
Escala / Scale 1:1
Formato / Format A4
Material / Material Cobre libre de oxígeno
Hoja/Sheet 1/1
Nº. POS01-01-01-01-04
POSEIDON
Conector
Este documento no podrá ser copiado o entregado a terceros sin el permiso escrito de ANTEC,S.A.U.
This document must not be copied or given to third party without the written permission of ANTEC,S.A.U.
antec

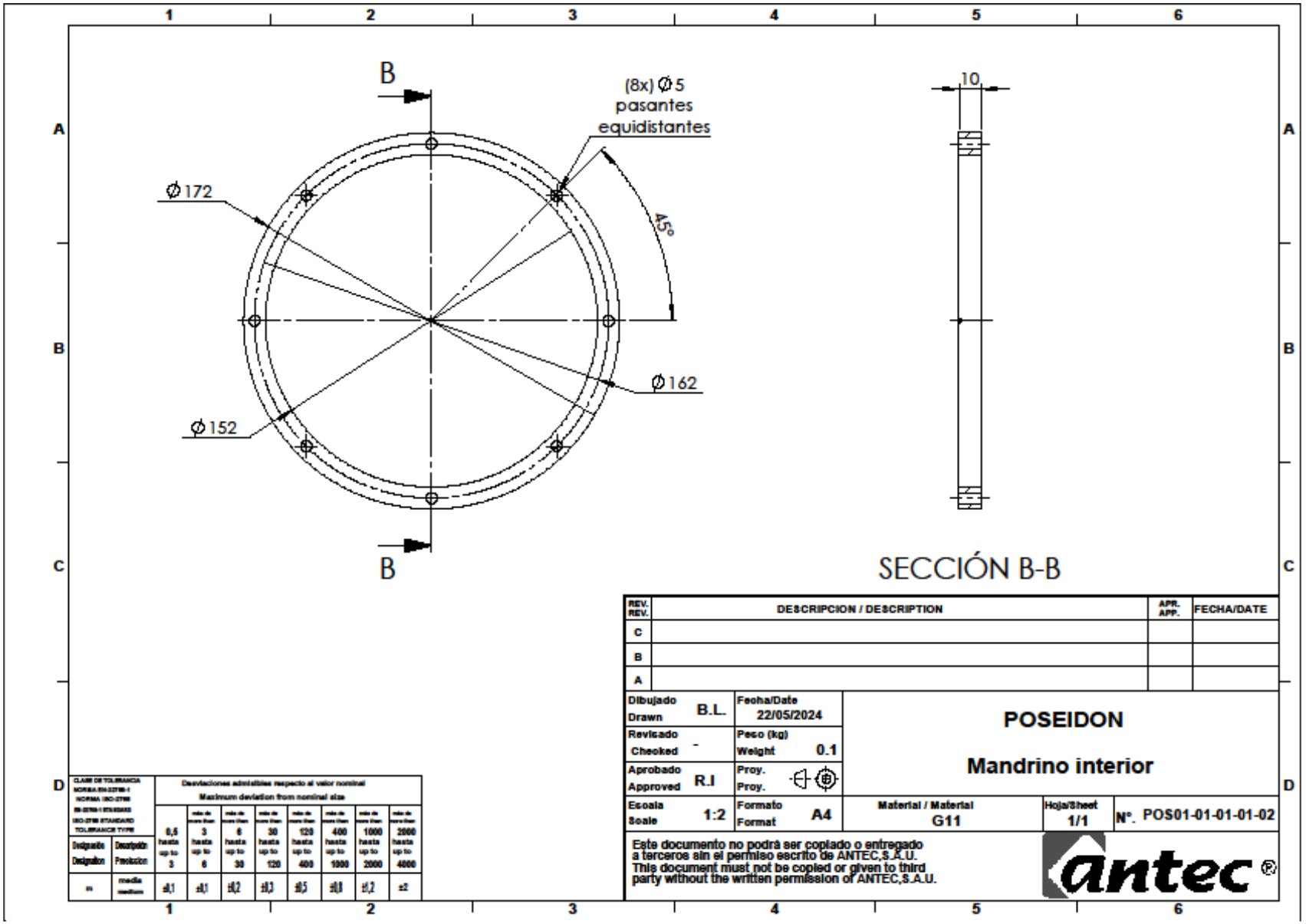

REV. REV.	DESCRIPCION / DESCRIPTION	APR. APP.	FECHA/DATE
C			
B			
A			

Dibujado / Drawn: B.L.	Fecha/Date: 22/05/2024	POSEIDON	
Revisado / Checked: -	Peso (kg) / Weight: 0.1	Mandrino interior	
Aprobado / Approved: R.I	Proy. / Proy.		
Escala / Scale: 1:2	Formato / Format: A4	Material / Material: G11	Hoja/Sheet: 1/1 — Nº. POS01-01-01-01-02

Este documento no podrá ser copiado o entregado a terceros sin el permiso escrito de ANTEC,S.A.U.
This document must not be copied or given to third party without the written permission of ANTEC,S.A.U.

antec®

CLASE DE TOLERANCIA / TOLERANCE TYPE	Desviaciones admisibles respecto al valor nominal / Maximum deviation from nominal size							
Designación / Designation	Descripción / Description	0,5 hasta 3	más de 3 hasta 6	más de 6 hasta 30	más de 30 hasta 120	más de 120 hasta 400	más de 400 hasta 1000	más de 1000 hasta 2000	más de 2000 hasta 4000
m	media / medium	±0,1	±0,1	±0,2	±0,3	±0,5	±0,8	±1,2	±2